Tectonics and hydrocarbon systems of the East Gobi basin, Mongolia

G. L. Prost

ABSTRACT

Mapping in the East Gobi basin, supplemented by seismic data, reveals a structural and burial history for basins adjacent to the Zuunbayan and Tsagaan Els oil fields. The tectonic framework was combined with available well and outcrop data to model the timing and magnitude of hydrocarbon generation.

Five structural episodes are recognized: (1) pre-Jurassic northeast-directed shortening that formed the tectonic fabric; (2) Middle Jurassic to Early Cretaceous rifting along northeast trends that formed the subbasins of the East Gobi basin; (3) late Early Cretaceous north-south shortening and inversion on existing normal faults; shortening caused left-lateral and reverse displacements on northeast-trending faults; (4) middle Cretaceous uplift and erosion, followed by (5) east-west shortening and right-lateral movement on northeast faults. Folds formed by inversion over Middle Jurassic–Early Cretaceous normal faults.

Modeling suggests that the bituminous member of the Zuunbayan Formation should be mature over large parts of the Unegt and Zuunbayan subbasins. Oil migrated from mature source areas toward several traps, including the Zuunbayan and Tsagaan Els fields. Modeling suggests that early oil (104–110 Ma) was generated in the Zuunbayan and Tsagaan Els area because of deep burial during the Cretaceous. Although generation began in the Early Cretaceous, peak generation in the Unegt subbasin occurred between 100 and 90 Ma. Generation continued at a decreasing rate up to the present day. Kerogen maturity (and oil field production) suggests that oil is the most likely product. Scoping calculations of hydrocarbon volumes generated indicate that the Unegt basin may have generated as much as 86 billion BOE.

INTRODUCTION AND PREVIOUS WORK

A tectonic evolution and hydrocarbon maturation history are proposed for the East Gobi basin, Mongolia, on the basis of new mapping,

Manuscript received April 30, 2003; provisional acceptance August 25, 2003; revised manuscript received October 23, 2003; final acceptance November 15, 2003.

DOI:10.1306/11150303042

AUTHOR

G. L. Prost ~ *ConocoPhillips Canada, 401 9th Ave. SW, Calgary, Alberta, Canada T2P 2H7; Gary.Prost@conocophillips.com*

Gary Prost received his Ph.D. in geology from the Colorado School of Mines and works for ConocoPhillips Canada on development of the Parsons Lake gas field, Northwest Territories. Over 28 years in the energy industry, he has worked for the U.S. Geological Survey, Superior Oil, Amoco, and Gulf Canada and is author of *Remote Sensing for Geologists* and *English–Spanish Glossary of Geoscience Terms*.

ACKNOWLEDGEMENTS

This work was supported by Gulf Canada (presently ConocoPhillips) and ROC Oil. Thanks are directed to ConocoPhillips, the Petroleum Authority Mongolia, and John Doran of ROC Oil for permission to publish and to use seismic and satellite data acquired or purchased by ROC/Gulf Canada. Invaluable field assistance was provided by Dadingiin Janchiv, and logistics support was provided by Mark Temple and Bill Childress at Zuunbayan. Discussions with Stephan Graham, Cari Johnson, and Randall Marrett were invaluable. Comments and suggestions by the manuscript reviewers (William DeMis, Stephan Graham, and Qingming Yang) are appreciated and improved the paper.

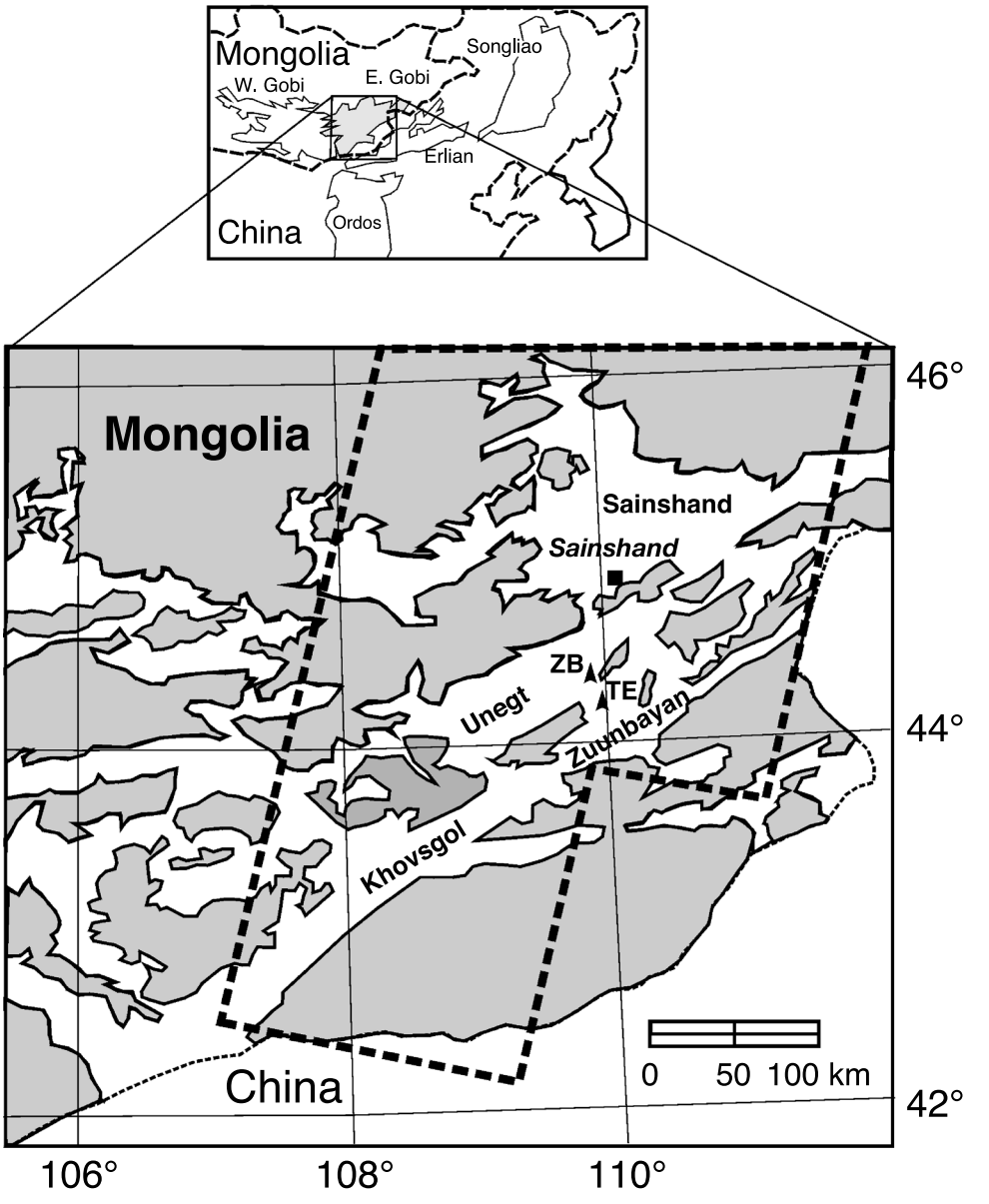

Figure 1. Index map showing the subbasins of southeastern Mongolia and the area described in this paper. TE is the Tsagaan Els field; ZB is the Zuunbayan field. Outline of satellite images used in this work are shown.

seismic, and geochemical data (Figure 1). This paper examines questions posed during exploration by Gulf Canada and ROC Oil in basins adjacent to the Zuunbayan and Tsagaan Els oil fields:

1. What structures can be expected in these basins, and what age are they?
2. Where are the best porosity and permeability reservoir rocks?
3. When did hydrocarbons generate, and where did they migrate?

The East Gobi basin contains thousands of meters of Mesozoic and younger sediments above a largely metamorphic basement. Several subbasins began forming in Jurassic time and were modified during subsequent tectonic episodes. The combination of thick section, surface structures, and seeps led to exploration interest.

The Zuunbayan oil field was discovered in 1941, when a well was drilled on a northeast-trending anticline containing surface oil seeps (Blechner, 1990). The source rock and reservoir are both Lower Cretaceous lacustrine sediments (Mongolian Petroleum Company and Exploration Associates International of Texas, 1990; Amory and Keller, 1995; Graham et al., 2001; Johnson, 2002). This was followed by discovery of the Southwest Zuunbayan field and Tsagaan Els fields, also in anticlines. Estimated oil in place at Tsagaan Els is 96 MMBO and at

Table 1. Data Sources and Previous Work

Hydrocarbon System	Khutorskoy and Yarmoluk, 1989	heat flow
	Blechner, 1990	production history and reserves
	Mongolian Petroleum Company and Exploration Associates International of Texas, 1990	source rock, field descriptions
	Yamamoto, et al., 1993	geochemistry
	Pentilla, 1994	reserve volumes
	Amory and Keller, 1995	source rock
	China National Petroleum Company, 1995	Chinese field analogs
	M. Porter, 1996, personal communication	Chinese field analogs
	Johnson, 2002	maturation modeling
Stratigraphy	Meyerhoff and Meyer, 1987	heavy oil; stratigraphy
	Lamb and Badarch, 1997	Paleozoic basins
	E. H. Davies, 1999, personal communication	palynology and depositional environments
	Johnson, 2002	Mesozoic lacustrine sequences
	Graham et al., 2001	stratigraphy
Tectonics	Tapponnier and Molnar, 1977	plate tectonic framework
	Hefu, 1986	plate tectonic framework
	Tapponnier et al., 1986	plate tectonic framework
	Peltzer and Tapponnier, 1988	plate tectonic framework
	Dewey et al., 1989	plate tectonic framework
	England and Molnar, 1990	plate tectonic framework
	Zhao et al., 1990	plate tectonic framework
	Everett et al., 1991	regional synthesis
	Pruner, 1992	paleomagnetic reconstructions
	Tseden et al., 1992	tectonic overview
	Chen et al., 1993	Asian tectonics prior to collision with India
	Ermikov, 1994	Cenozoic tectonics
	Hendrix et al., 1994	tectonics and sedimentation
	Zhao et al., 1990	paleomagnetic reconstructions
	Traynor and Slaydon, 1995	tectonics and sedimentation
	Dobretsov et al., 1996	Cenozoic tectonics
	Graham et al., 1996	tectonics and sedimentation
	Hendrix et al., 1996	tectonics and sedimentation
	Zhao et al., 1990	paleomagnetic reconstructions
	Lamb et al., 1999	Cenozoic tectonics
	Davis et al., 2000	pre-Jurassic metamorphic core complexes
	Johnson et al., 2001	tectonics and sedimentation
	Graham et al., 2001	tectonics and sedimentation
	Johnson, 2002	tectonics and sedimentation

Zuunbayan is 60 MMBO. The oil averages 28° API and is waxy (30–35% paraffin) and biodegraded (Meyerhoff and Meyer, 1987; Traynor and Sladen, 1995; M. Porter, 1996, personal communication). Reservoirs consist of sandstones with a high percentage of volcanic fragments and clays that hinder production. For this reason, it is desirable to find high-porosity (quartz-rich) reservoir units. The eastern basins (East Gobi, Tamtsag, and Choibalsan) could contain in the range of 162–1770 million BOE, with the most likely [sic] value around 885 MMBO (Pentilla, 1994).

Previous work (Table 1) describes the stratigraphy of the East Gobi basin as consisting primarily of sands and shales deposited in Jurassic and Cretaceous alluvial,

fluvial, and lacustrine environments. Thin Tertiary continental deposits overlie the Mesozoic units. Alternating periods of tectonic shortening and extension related to the interplay between the Asian, Indian, and Pacific tectonic plates modified the basin structure such that faults show normal, reverse, and strike-slip offsets, and folding is widespread. Structural development influenced sedimentation (facies, thickness, and source rock distribution), maturation of source rock (burial history and heat flow), and hydrocarbon accumulation (traps).

GEOLOGIC SETTING

Stratigraphy

Paleozoic volcanic arc-related marine siliciclastics and carbonates of the Tavan Tolgoy sequence are metamorphosed over much of the area and form economic basement in the East Gobi basin (Traynor and Sladen, 1995; Lamb and Badarch, 1997; Graham et al., 2001). Basement is unconformably overlain by 1000–4000 m (3300–13,000 ft) of Middle Jurassic to Tertiary alluvial, fluvial, and lacustrine sediments (Meyerhoff and Meyer, 1987). The Middle–Upper Jurassic Khamar Khoovor Formation consists of as much as 750 m (2500 ft) of braided fluvial channel sandstones and lacustrine-deltaic-swamp-related shales unconformably overlain by as much as 200 m (600 ft) of braided fluvial sandstones and conglomerates and minor lacustrine shales of the Sharlyn Formation of Tithonian–Kimmeridgian age (Graham et al., 2001). The Sharlyn Formation grades upward into a 300–700-m (1000–2300-ft)-thick, dominantly shale section interbedded with dark gray sandstones and conglomerates, siltstones, bright-red tuffs, and a vesicular basalt. This unit, the Valanginian Tsagaan Tsav Formation, fines upward from alluvial fan to braided stream to probable flood-plain and lacustrine facies (Graham et al., 2001; Johnson, 2002). The Tsagaan Tsav Formation is the reservoir unit at Tsagaan Els and Zuunbayan fields, where it is a lithic sandstone. The Zuunbayan Formation, consisting of as much as 970 m (3200 ft) of sands and minor interbedded shales and tuffs, was deposited during Hauterivian to Albian time. Palynomorphs suggest nonmarine to paralic depositional environments (E. H. Davies, 1999, personal communication). This unit has a characteristic bituminous shale at its base and coals, basalt flows, and channel sandstones in the upper part of the section. The Tsagaan Tsav and Zuunbayan together are upward of 1500 m (4900 ft) thick. An unconformity separates the Lower from the Upper Cretaceous. The Cenomanian Sainshand Formation consists of red sandstones, conglomerates, and claystones. It is, in turn, overlain by the Santonian–Turonian Bayanshiree Formation, mainly red and gray shales with occasional coarse fluvial channel sandstones (Graham et al., 2001; Johnson, 2002). In places, the Bayanshiree Formation is covered by the Santonian to Campanian Baruungoyot Formation and Campanian–Maastrichtian Nemegt Formation. Both of these units are dominantly coarse clastics infilling lake basins (Stratigraphic Services International et al., 1991). The section is topped by Tertiary thin-bedded fine to coarse alluvium.

Basins

The term East Gobi basin applies to four subbasins in an area of east-central Mongolia extending roughly 700 km (400 mi) east-west by 300 km (200 mi) north-south and having a similar stratigraphic section (Figure 2). These subbasins contain a relatively thick section above the Paleozoic, based on gravity and seismic data purchased or acquired by ROC Oil and Gulf Canada. The presence of granitic units around basin margins, indicated by light-colored units on satellite imagery or shown on published maps (Ositsev, 1951; Pershitkin et al., 1952; Yanshin, 1989; Petroleum Authority of Mongolia, date unknown), suggests that quartz-rich (and presumably good-porosity) reservoir units might exist in these subbasins.

Unegt Subbasin

The northeast-oriented Unegt subbasin is roughly 35–40 km (22–25 mi) wide and nearly 120 km (75 mi) long, narrowing on both ends to about 10 km (6 mi) wide. A range of structures exists in the basin, from anticlines to domes. At least two basin deeps are indicated on seismic data: just north of the Zuunbayan field (depths to top Paleozoic of as much as 3000 m [9800 ft]) and along the north flank of the basin (depths to 4000 m [13,000 ft]). Gravity also suggests that the north flank of the basin contains the thickest section (Mongolian Petroleum Company, 1992). Granitic outcrops encountered during field mapping northeast of Hutuul Uus provide encouragement that reservoir units in that area may contain fewer lithic fragments and thus, better porosity than encountered in most wells and outcrops. Satellite images and aerial photographs show an

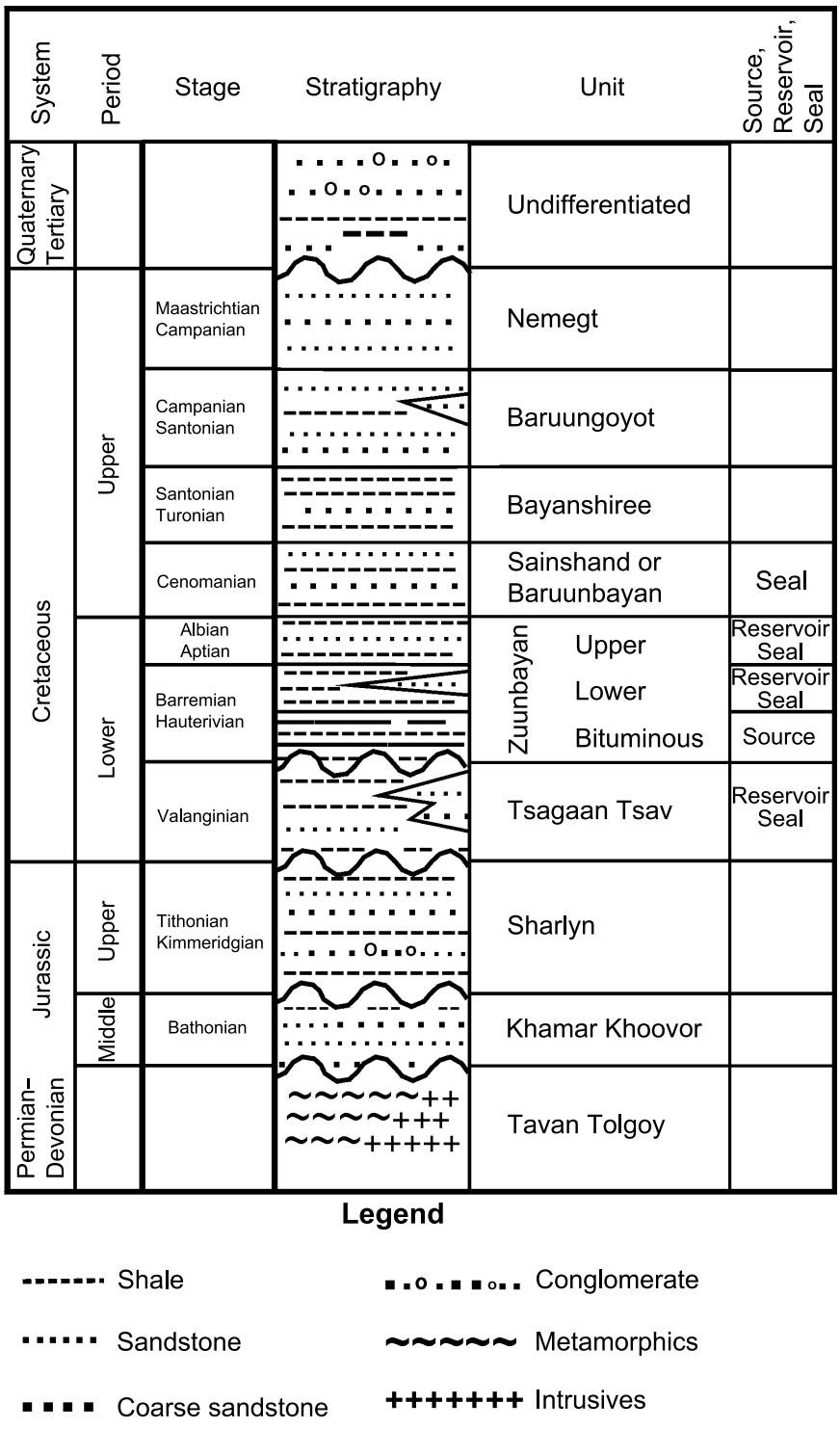

Figure 2. Stratigraphic column of the East Gobi basin. Source, reservoir, and seal are shown. Modified after Mongolian Petroleum Company and Exploration Associates International of Texas (1990) and Stratigraphic Services International et al. (1991).

abundance of folds at the surface along the flanks of this subbasin (Figure 3).

Zuunbayan Subbasin

The northeast-trending Zuunbayan subbasin is roughly 20 km (12 mi) wide and 100 km (60 mi) long and merges with the Khovsgol subbasin to the southwest. The basin is poorly defined, except in the northeast portion where seismic data exist. Gravity data (Mongolian Petroleum Company, 1992) suggest there are at least two deep areas, one surrounding the Tsagaan Els structure and the other about 50 km (30 mi) southwest of Tsagaan Els. A preliminary depth conversion of ROC Oil

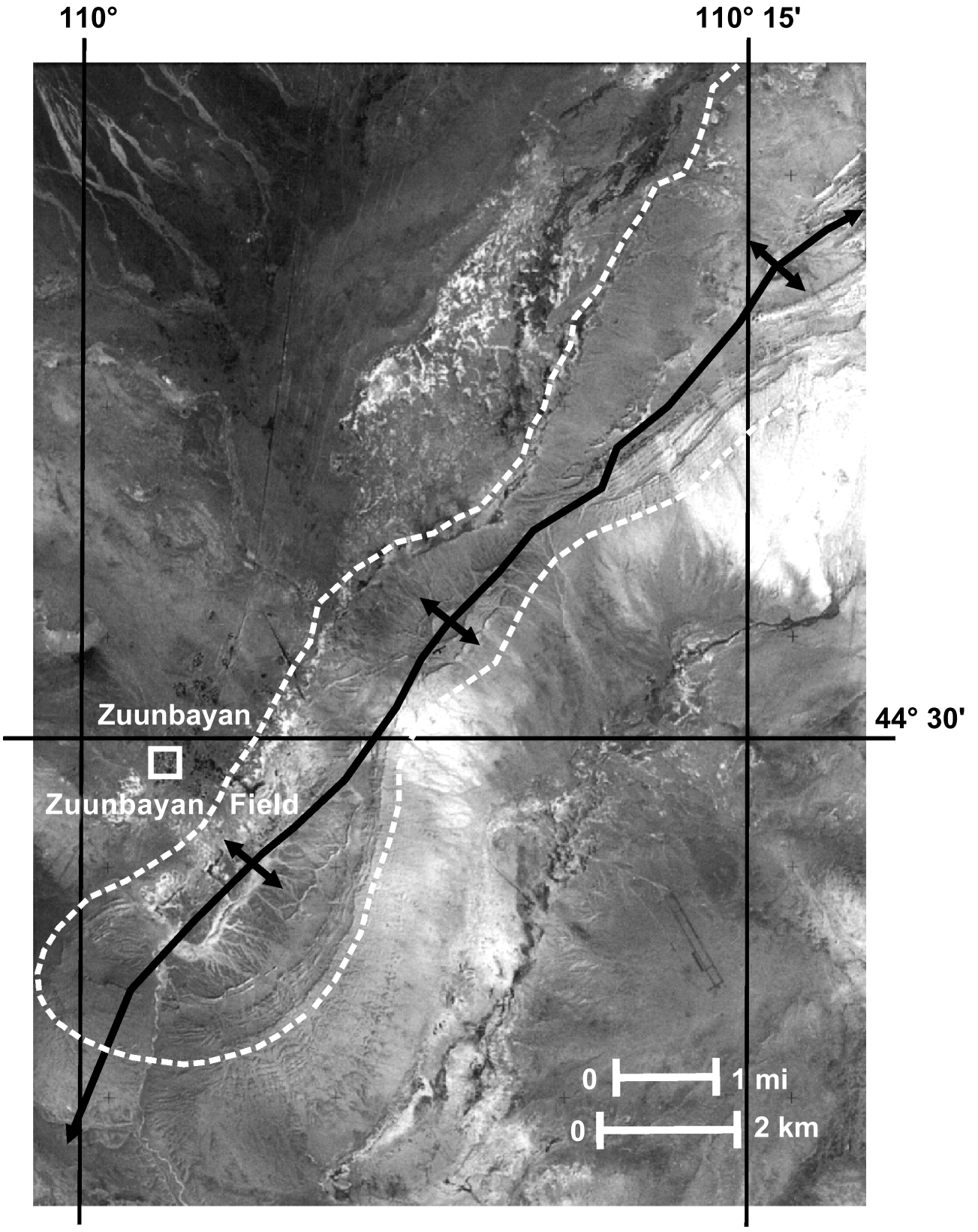

Figure 3. Landsat Thematic Mapper image of the Zuunbayan field and anticline. This northwest-verging structure is a result of post-middle Cretaceous inversion over an earlier normal fault. Resolution is roughly 30 m.

and Gulf Canada–owned seismic lines near Tsagaan Els suggests that the basin contains as much as 4000 m (13,000 ft) of post-Paleozoic section. Outcrops of Permian(?) age granites along the northeast and southern margin of this basin suggest that quartz-arenite reservoir may exist in the subsurface in this part of the basin. Public-domain satellite imagery purchased and enhanced by ROC Oil and Gulf Canada shows anticlines as much as 5 km (3 mi) long and 1–2 km (0.6–1.2 mi) wide, as well as uplifts where older units outcrop in the Tertiary–Quaternary cover (Figure 4).

Khovsgol Subbasin

The Khovsgol subbasin is the southwest extension of the Zuunbayan subbasin. It is elongated roughly east-west, is 17–35 km (11–22 mi) wide, and is at least 150 km (93 mi) long. The town of Khovsgol lies on the southern flank of a high block in the east-central basin. Seismic line WS91-EG-3 shows a low in the northern (~43°35′N, 108°45′E) part of the basin. The surface geologic map (Yanshin, 1989) shows a few widely scattered granite outcrops and one large area of granite along the southeastern flank of the basin, suggesting that quartz-rich reservoir may exist in the subsurface of that area. Satellite mapping shows few surface structures in this basin (Figure 5).

Sainshand Subbasin

The Sainshand subbasin covers a large area (50–150 km [31–93 mi] east-west; 40–100 km [25–62 mi] north-south) north of the town of Sainshand. Gravity data (Mongolian Petroleum Company, 1992) suggest that there are at least two lows in the basin, one centered about 35 km northwest of Sainshand and the other (confirmed by seismic line WS91-EG-6) centered 55 km north of Sainshand. In addition, seismic lines WS91-EG-1 and WS91-EG-6 show a basin deep located approximately 30–60 km (18–37 mi) northeast of town. Satellite mapping shows several long (as much as 12.5 km [8 mi]), narrow east-northeast–trending anticlines along the southern flank of the basin and a few large folds in the central part of the basin (Figure 6).

GULF CANADA AND ROC OIL WORK PROGRAM

A large area of the East Gobi basin was mapped by the author in reconnaissance fashion before focusing on the Unegt and Zuunbayan subbasins around the Tsagaan Els and Zuunbayan fields. Five Landsat Thematic Mapper images, acquired during January 1989 and September 1990 and 1995, were evaluated during early 1998 at a scale of 1:250,000 as false color composites and as edge-enhanced black and white prints (Figure 1). Ten subscenes in areas of interest were interpreted at 1:100,000 (Figure 3). Finally, black and white Russian stereo airphotos at a scale of 1:32,000 were interpreted in critical areas, and the detail was added to the satellite-based mapping.

Images were interpreted for all indications of structure and stratigraphy and compiled on 1:100,000 topographic base maps. Field mapping and kinematic measurements were collected by the author and J. Janchiv (Bayan Oil) during September 1998 to validate satellite and airphoto mapping and to determine the structural style in the area. Cross sections at three locations across the basin illustrate the expected structural style based on surface mapping (Landsat, airphoto, and field measurements) and seismic and gravity data (Figures 7, 8, 9).

Well logs, cuttings, outcrop samples, and a review of the literature provided information on the stratigraphic section, potential source rocks, and reservoir characteristics. This was supported by field observations, and these data served as input for the hydrocarbon systems model.

STRUCTURE

Folds were mapped using imagery, airphotos, seismic lines, and field measurements. Five tectonic episodes are expressed in structures in the East Gobi basin. Pre-Jurassic northeast-directed shortening is defined by east-northeast–oriented left-lateral faults and north-northwest–trending right-lateral faults in Precambrian and Paleozoic metasediments. Middle Jurassic to Early Cretaceous rifting (north-south extension) formed the original basins in this area. In late Early Cretaceous, north-south shortening and inversion occurred on preexisting faults, resulting in left-lateral and reverse offsets. After the middle Cretaceous unconformity, there was renewed sedimentation and right-lateral displacement along northeast faults. Post-Late Cretaceous east-west shortening is recognized.

The dominant surface fault trend throughout the East Gobi basin is oriented northeast to east-northeast. Left-lateral offset is described on northeast-trending faults in southeastern Mongolia (Lamb et al.,1999; Yue and Liou, 1999; Graham et al., 2001; Johnson, 2002). Some workers propose 185–235 km (115–145 mi)

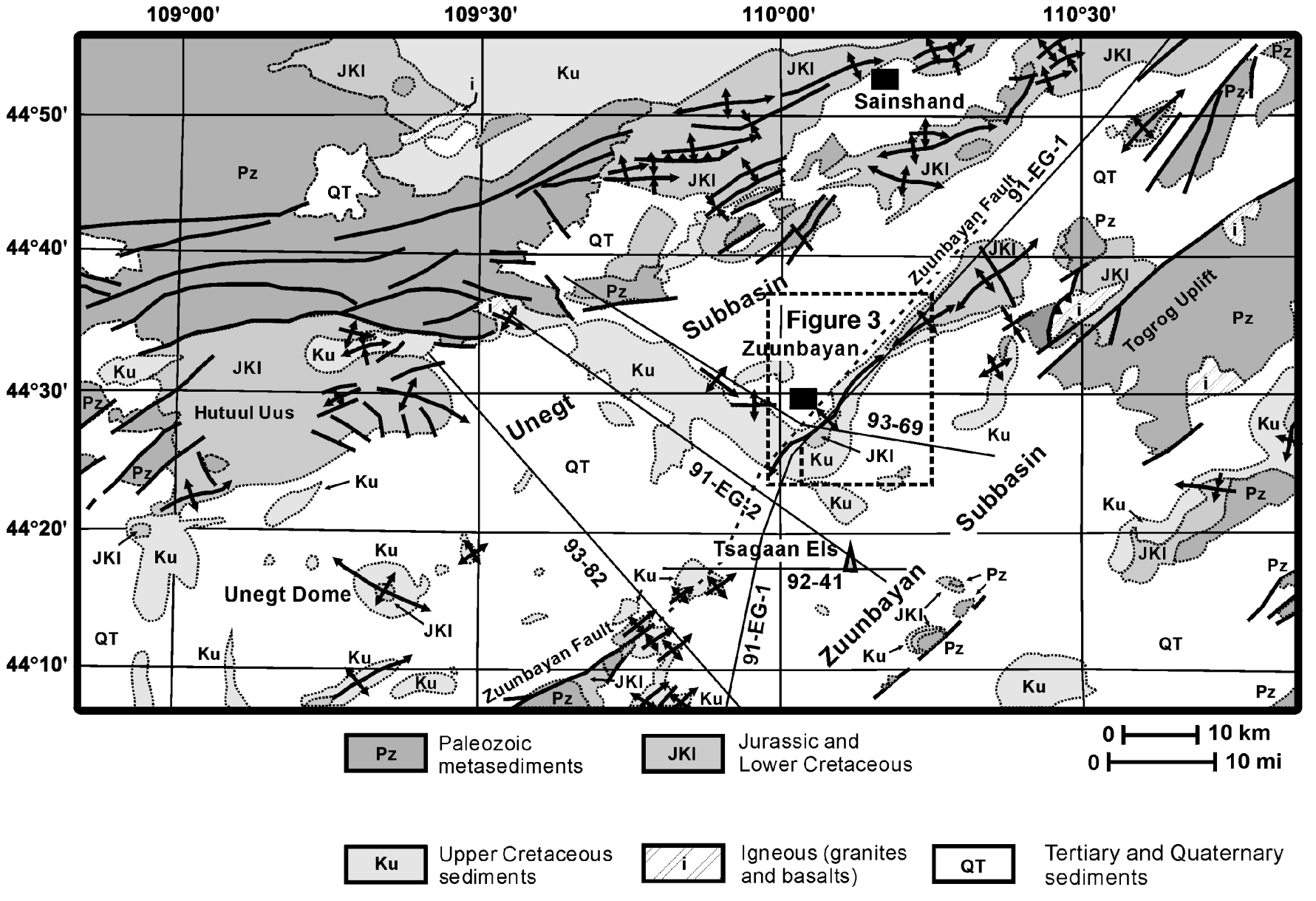

Figure 4. Geology of the Unegt subbasin derived from satellite, airphoto, and field mapping. Seismic lines used in this paper are shown. Stratigraphic ages from Ositsev (1951), Pershitkin et al. (1952), Yanshin (1989), and the Petroleum Authority of Mongolia (date unknown).

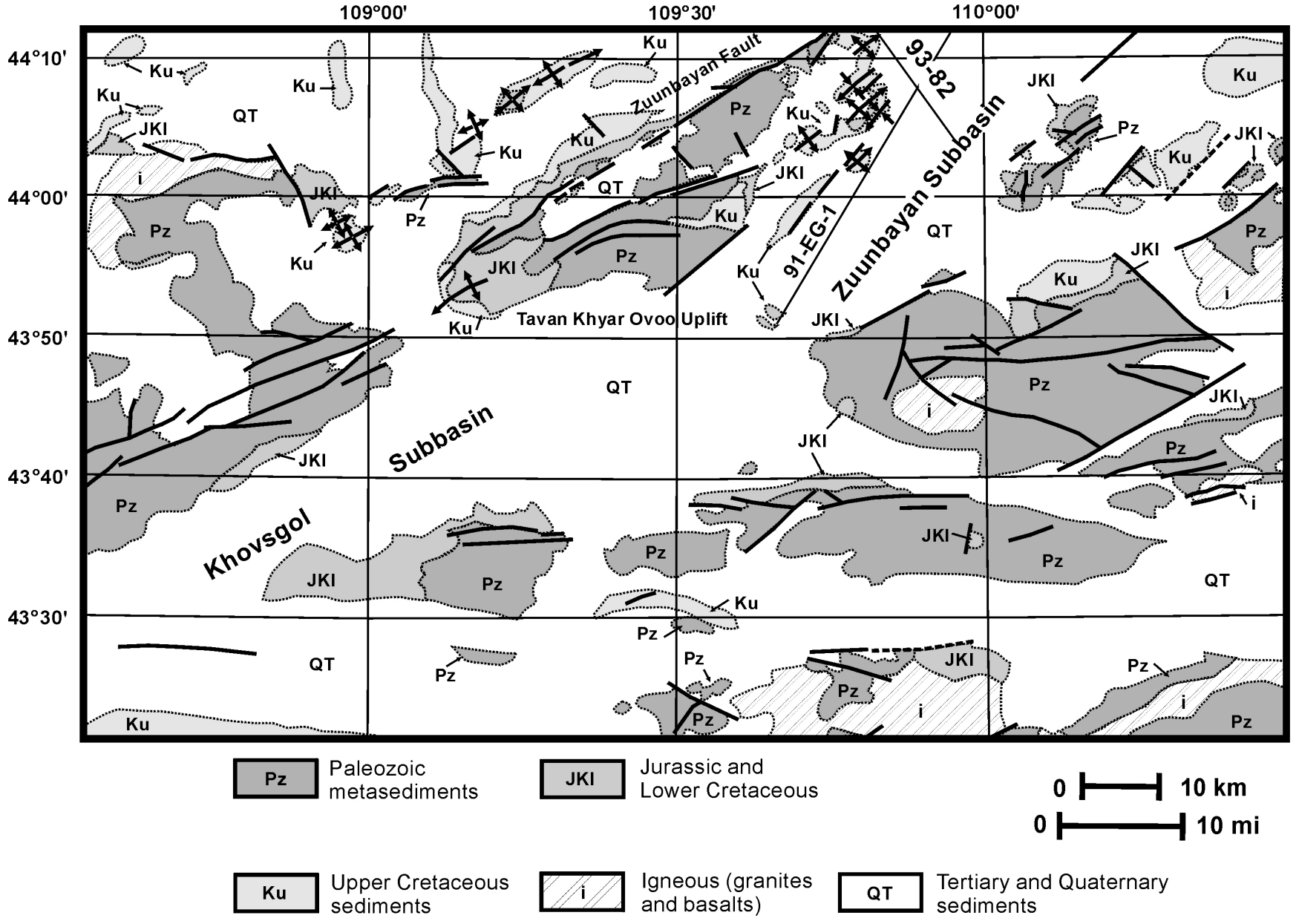

Figure 5. Geologic map of the Zuunbayan and Khovsgol subbasins derived from satellite, airphoto, and field mapping and showing seismic lines referred to in this paper. Stratigraphic ages from Ositsev, 1951; Pershitkin et al., 1952; Yanshin, 1989; and the Petroleum Authority of Mongolia, date unknown.

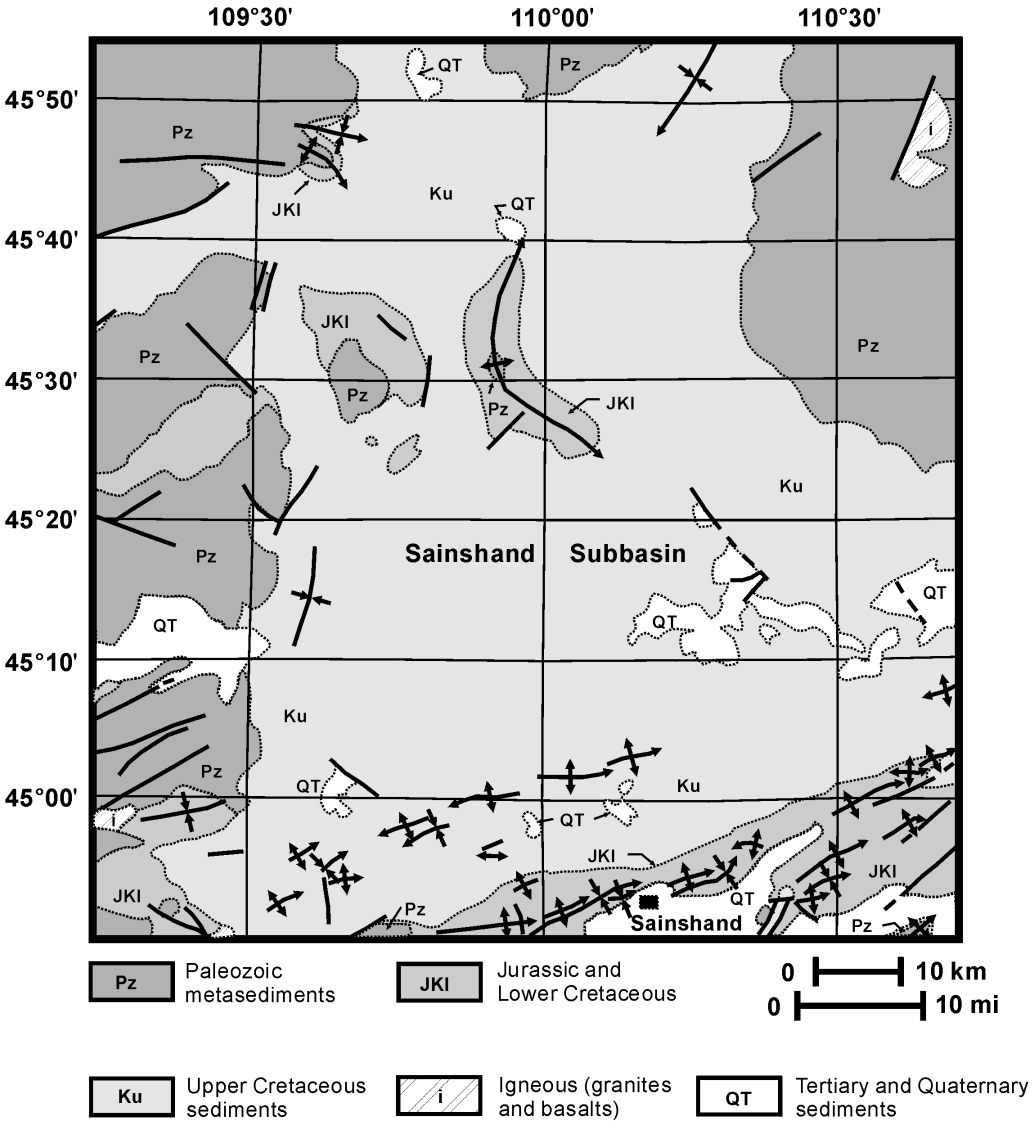

Figure 6. Geologic map of the Sainshand subbasin derived from satellite and field mapping. Stratigraphic ages from Ositsev (1951), Pershitkin et al. (1952), Yanshin (1989), and the Petroleum Authority of Mongolia (date unknown).

left-lateral offset in the East Gobi basin prior to the Late Cretaceous (Lamb et al.,1999). Approximately 400 km (250 mi) left-lateral offset is estimated on major faults primarily during the Oligocene (Yue and Liou, 1999). Triassic displacement is suggested based on Ar/Ar dating of synkinematic minerals (Graham et al., 2001). This suggestion is consistent with Late Triassic to Early Jurassic north-south shortening in northern China described by Davis et al. (2000). Middle Jurassic through Early Cretaceous (155–125 Ma) northwest-southeast extension in south-central Mongolia was followed by late Early Cretaceous transpression (110–95 Ma; Lamb et al., 1999; Graham et al., 2001; Johnson et al., 2001).

Field mapping in the Unegt and Zuunbayan subbasins found northeast-oriented basin-bounding faults with components of normal, reverse, and strike-slip offset (Figures 10, 11). Kinematic indicators, including fault-plane orientations, striations, and lineations, were measured on multiple fault planes at each field site. At several locations, two solutions are required to avoid simultaneous shortening and extension in the same direction. A review of these kinematic measurements indicates that reverse faults are roughly parallel with the strike-slip faults and have ''significant and consistent oblique movement, [which] might mean that they are reactivations of preexisting features...'' (Randall Marrett, 1998, personal communication).

Whereas these northeast faults have previously been described as left-lateral (e.g., Johnson, 2002), right-lateral offset is also interpreted from kinematic data on these

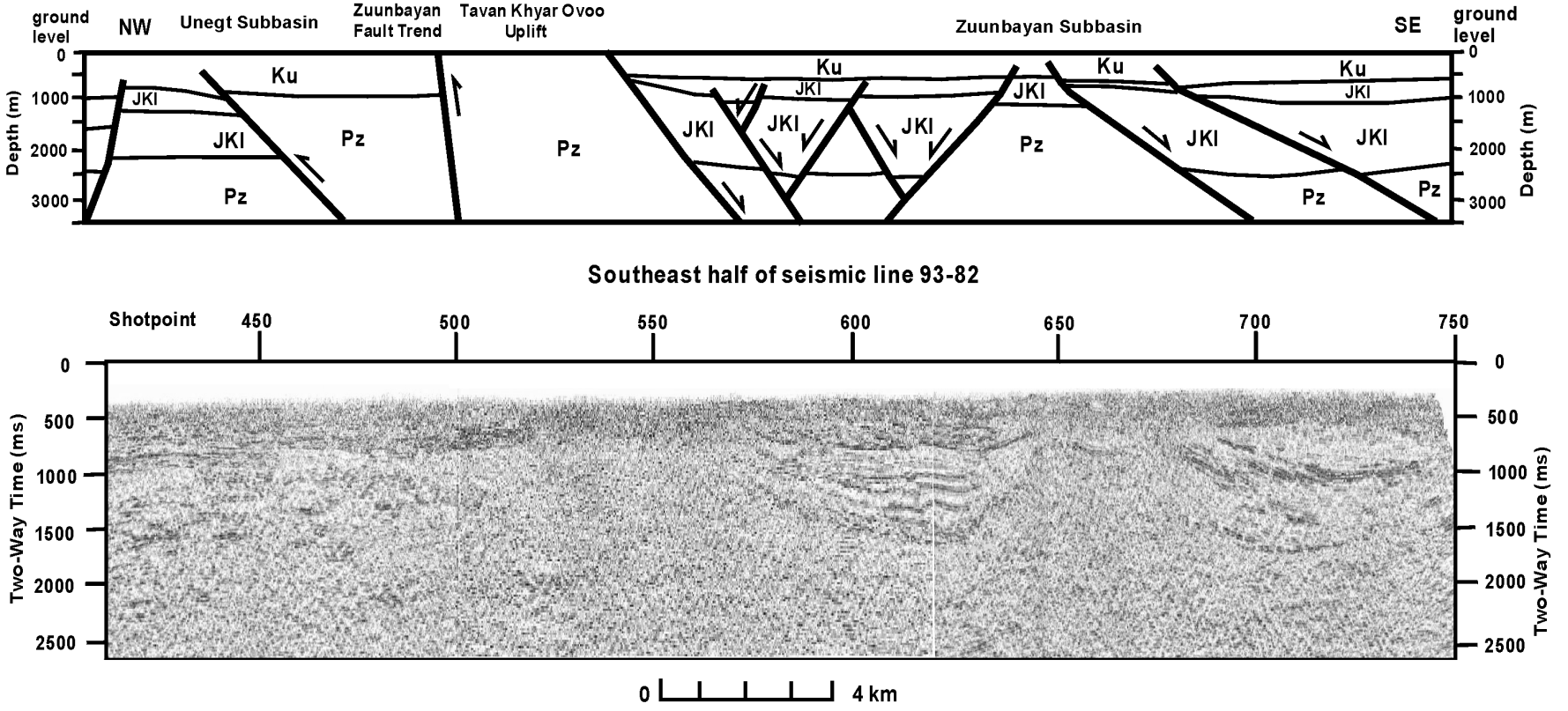

Figure 7. Northwest-southeast cross section along the southeast half of seismic line 93-82 (see Figure 4 for location). Structure is dominantly extensional in this part of the Zuunbayan subbasin and shows uplift and inversion in the Unegt subbasin. Pz = Paleozoic metasediments; JKl = Jurassic and Lower Cretaceous units; Ku = sediments of Upper Cretaceous age; QT = sediments of Tertiary and Quaternary age.

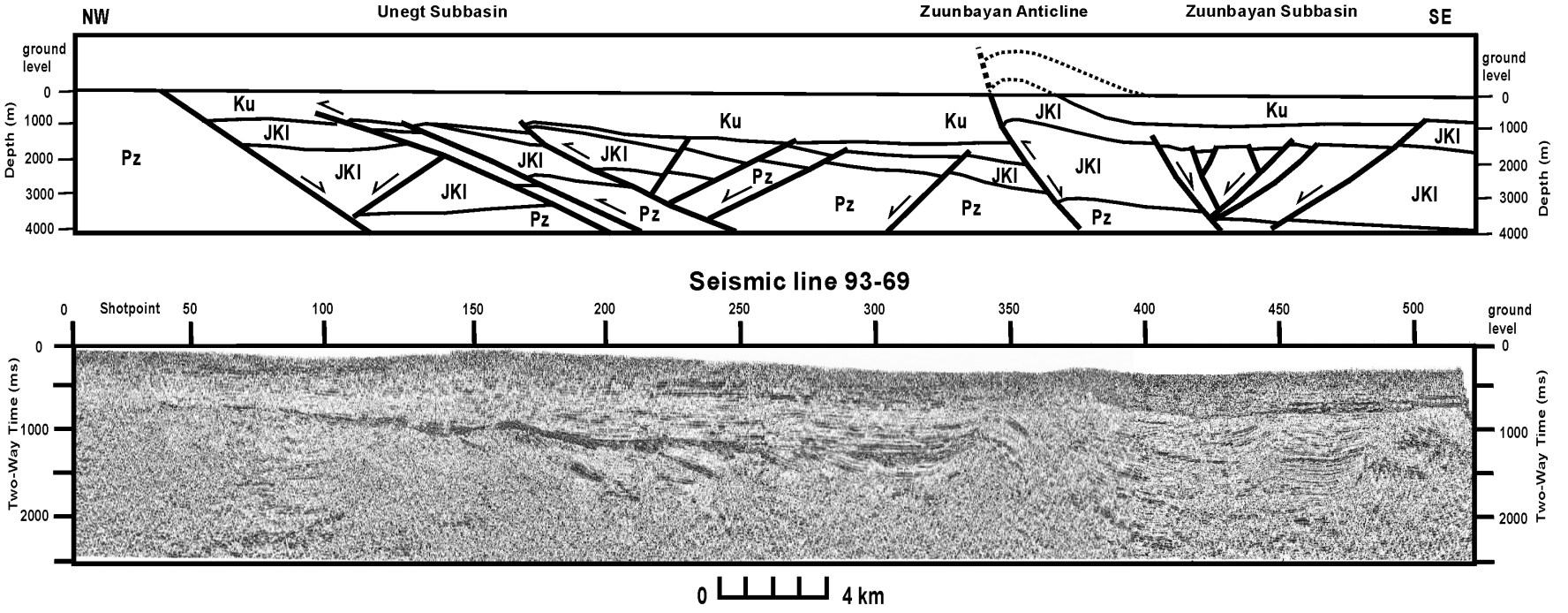

Figure 8. Northwest-southeast cross section along seismic line 93-69 (see Figure 4 for location). Inverted structures can be seen at and north of the Zuunbayan anticline; extensional structures are seen to the southeast. Pz = Paleozoic metasediments; JKl = Jurassic and Lower Cretaceous units; Ku = sediments of Upper Cretaceous age; QT = sediments of Tertiary and Quaternary age.

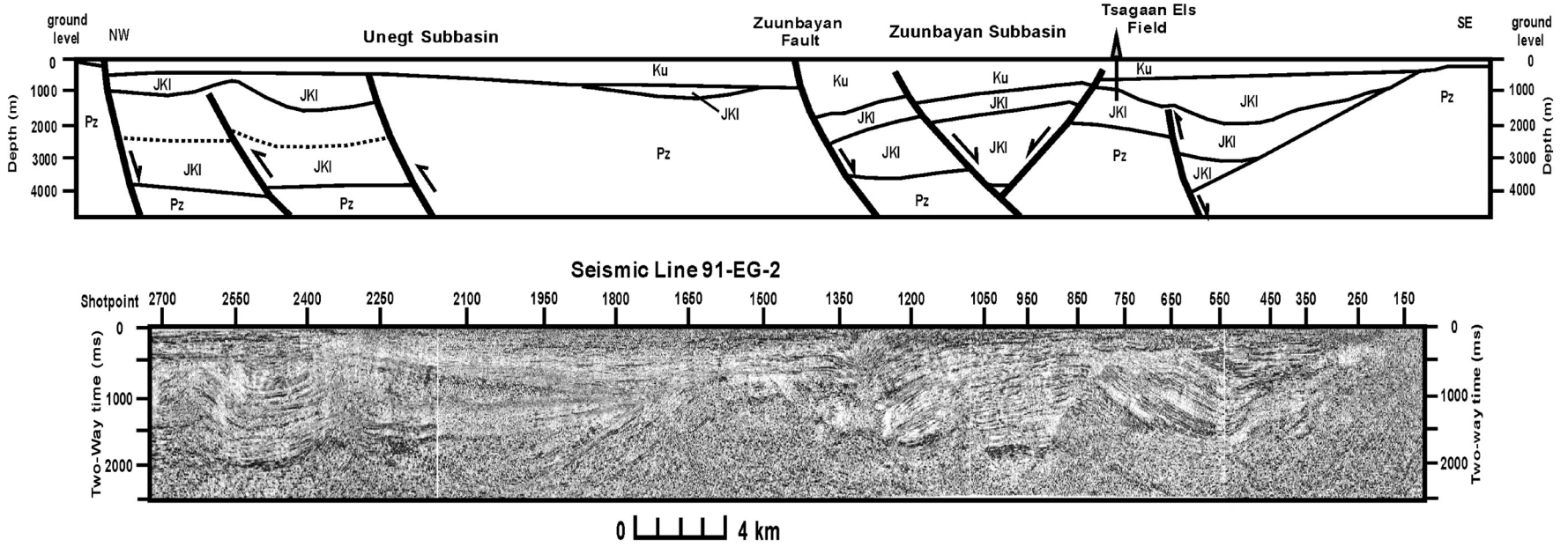

Figure 9. Northwest-southeast cross section along seismic line 91-EG-2 (see Figure 4 for location). Structure is dominantly extensional in the Zuunbayan subbasin, and shortening and inversion can be seen in the Unget subbasin. Pz = Paleozoic metasediments; JKl = Jurassic and Lower Cretaceous units; Ku = sediments of Upper Cretaceous age; QT = sediments of Tertiary and Quaternary age.

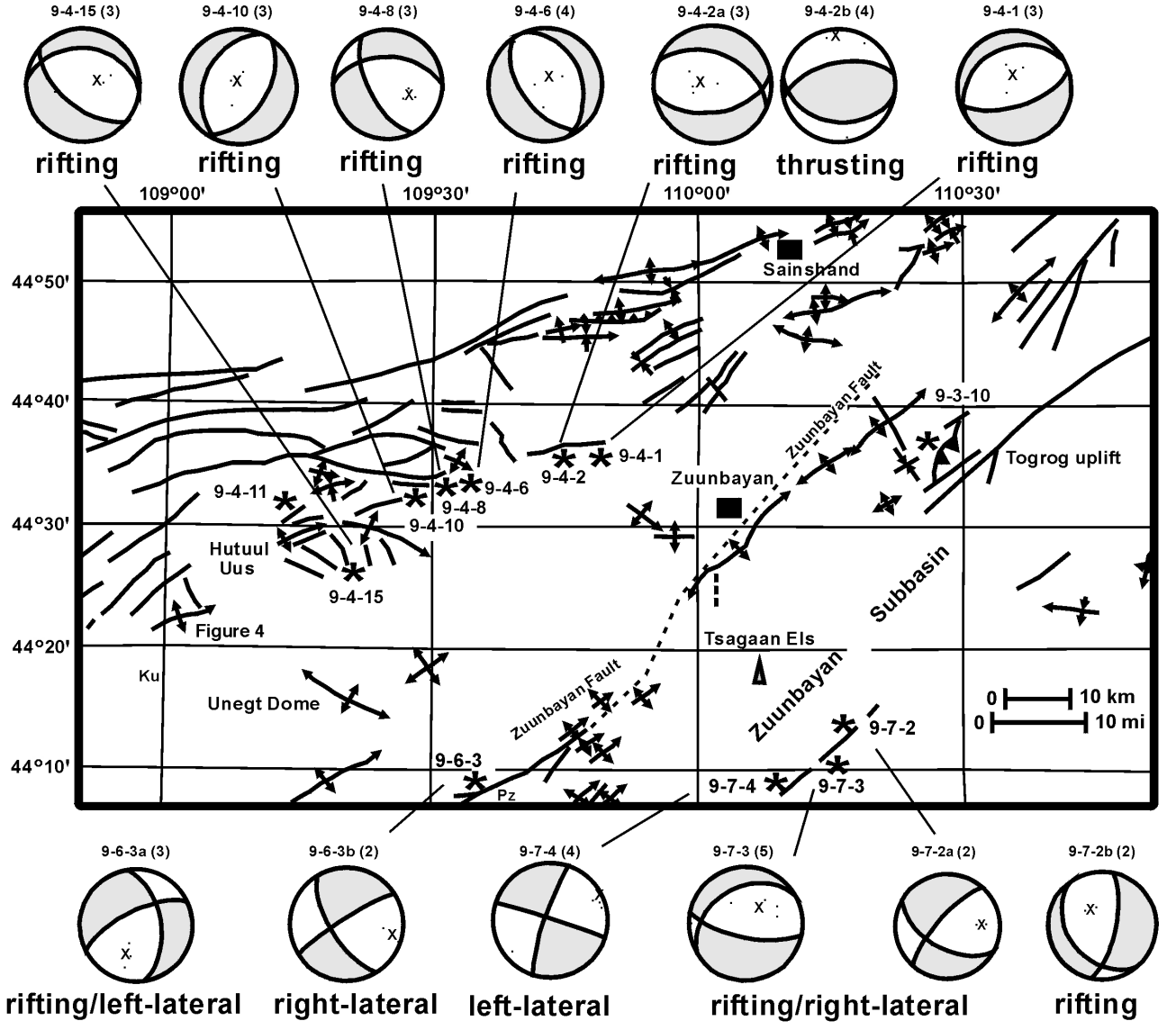

Figure 10. Kinematics of the Unegt and northern Zuunbayan subbasins. Pseudofocal mechanism solutions are given for field sites indicated on the figure. Some sites, such as 9-4-2 and 9-6-3, indicate multiple periods of deformation. Focal mechanism solutions use the lower hemisphere projection of a Schmidt net to indicate shortening axis and principal fault planes (Marrett and Allmendinger, 1990). The shortening field is white on the beach balls; extension fields are shaded. Shortening axis (σ_1, the maximum compression direction) is shown as an "x," and shortening poles are shown. A near-vertical shortening axis indicates rifting; a near-horizontal shortening axis indicates either thrusting or strike slip. The number of measurements at each site is shown in parentheses next to the location name.

faults in rocks as young as Late Cretaceous. Northeast-trending reverse faults with left-lateral offset show north-northwest to north-south shortening. Northeast normal and right-lateral faults indicate north-south extension (Figure 12). Northeast-trending faults are shown to have both right-lateral and left-lateral offsets. Seismic data (e.g., line GWS-91-EG-2) show northeast normal faulting followed by sedimentation and inversion during the Early Cretaceous (Figure 13). The Tsagaan Els structure is a tilted normal fault-bounded block with evidence of shortening prior to the middle Cretaceous unconformity (Figure 14). Seismic data also show that the southeast-dipping Zuunbayan fault has displacement that ranges along strike from normal (down to the southeast) to reverse. Normal and reverse offset along a single fault (e.g., Zuunbayan fault) can be caused only by strike slip, but

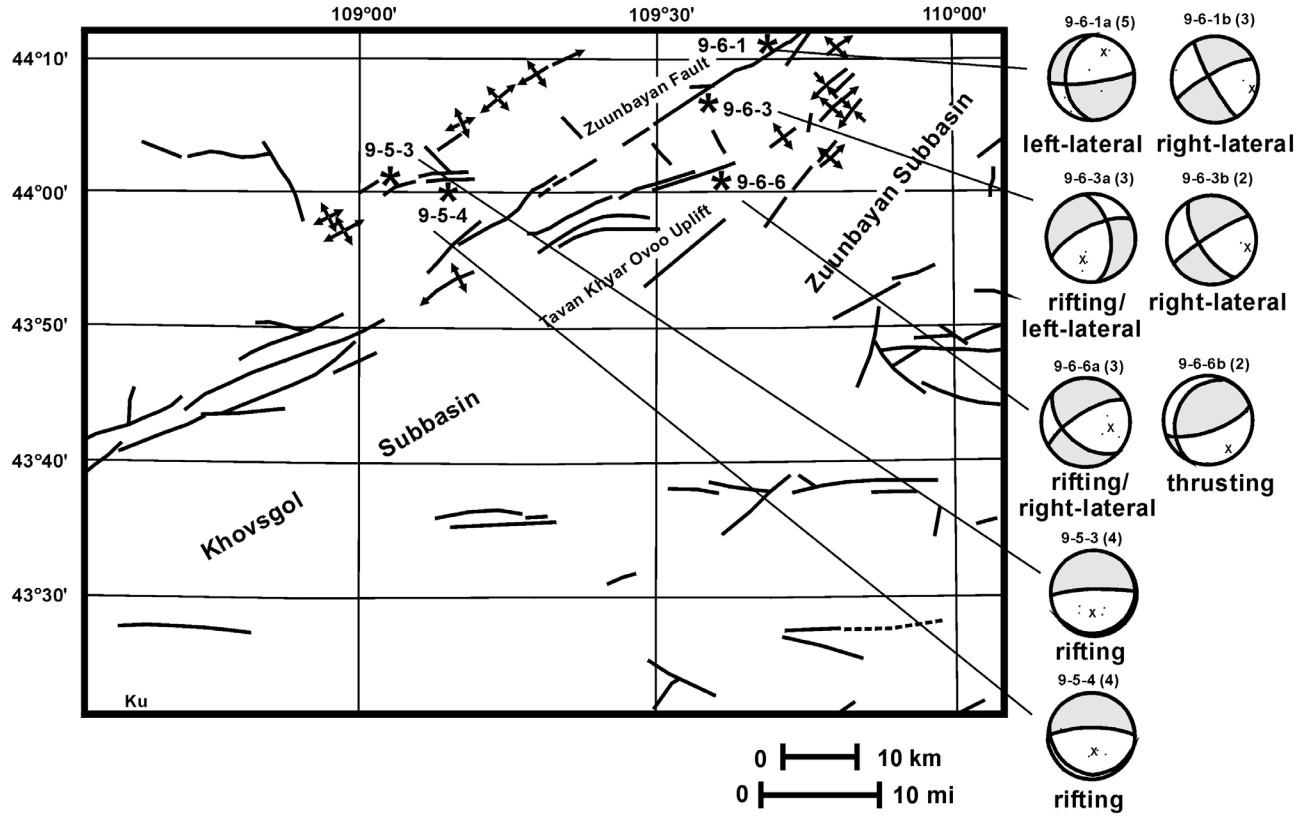

Figure 11. Kinematics of the Zuunbayan subbasin keyed to field sites. Sites such as 9-6-1, 9-6-3, and 9-6-6 suggest multiple periods of deformation. See Figure 10 for explanation of symbols.

taken together, these apparent contradictions may be best resolved by invoking more than one tectonic episode (for example, site 9-6-3, Figure 10).

An east-northeast tectonic fabric was inherited from pre-Jurassic structures. Pre-Jurassic faults had left-lateral offsets along east-northeast faults and right-lateral offsets along north-northwest faults, indicating northwest-southeast extension. Middle Jurassic–Early Cretaceous normal faulting formed the East Gobi subbasins along dominantly northeast-trending faults. Although areas to the south continued to experience southeast-northwest extension (Webb et al., 1999; Davis et al., 2000; Johnson et al., 2001), kinematic measurements indicate that the Unegt and Zuunbayan subbasins of the East Gobi basin underwent essentially north-south extension at this time. This extension was followed by late Early Cretaceous north-south shortening and resultant reverse and left-lateral displacement along northeast trends.

Seismic data suggest a reorganization of regional tectonics during the middle Cretaceous erosional event. Renewed extension and reactivation of basin-bounding normal faults, as seen by continued deposition in existing basins, occurred simultaneously with right-lateral displacements along northeast-trending faults (Dewey et al., 1989). Most Late Cretaceous and younger units are undeformed or gently dipping. Locally, however, Late Cretaceous sedimentation was followed by inversion (lines 92-41 and GWS-91-EG-1; Figures 13, 15). The Zuunbayan structure was formed by structural inversion after the Late Cretaceous was deposited. Late Cretaceous east-west shortening also caused right-lateral offsets along the northeast-trending basin-bounding faults.

Fault kinematic indicators, the age of units cut by faulting, and crosscutting relationships in the Zuunbayan and Unegt subbasins (Table 1) reveal at least four tectonic episodes (Figure 12; Table 2). A fifth episode, present-day shortening in adjacent parts of Mongolia and China, is oriented roughly east-west (Rapp et al., 1985).

The driver for changing maximum horizontal compressive stresses through time is uncertain, but several mechanisms have been mentioned (Graham et al., 2001; Johnson, 2002). Among these is the proposal that changes in shortening direction from north-south

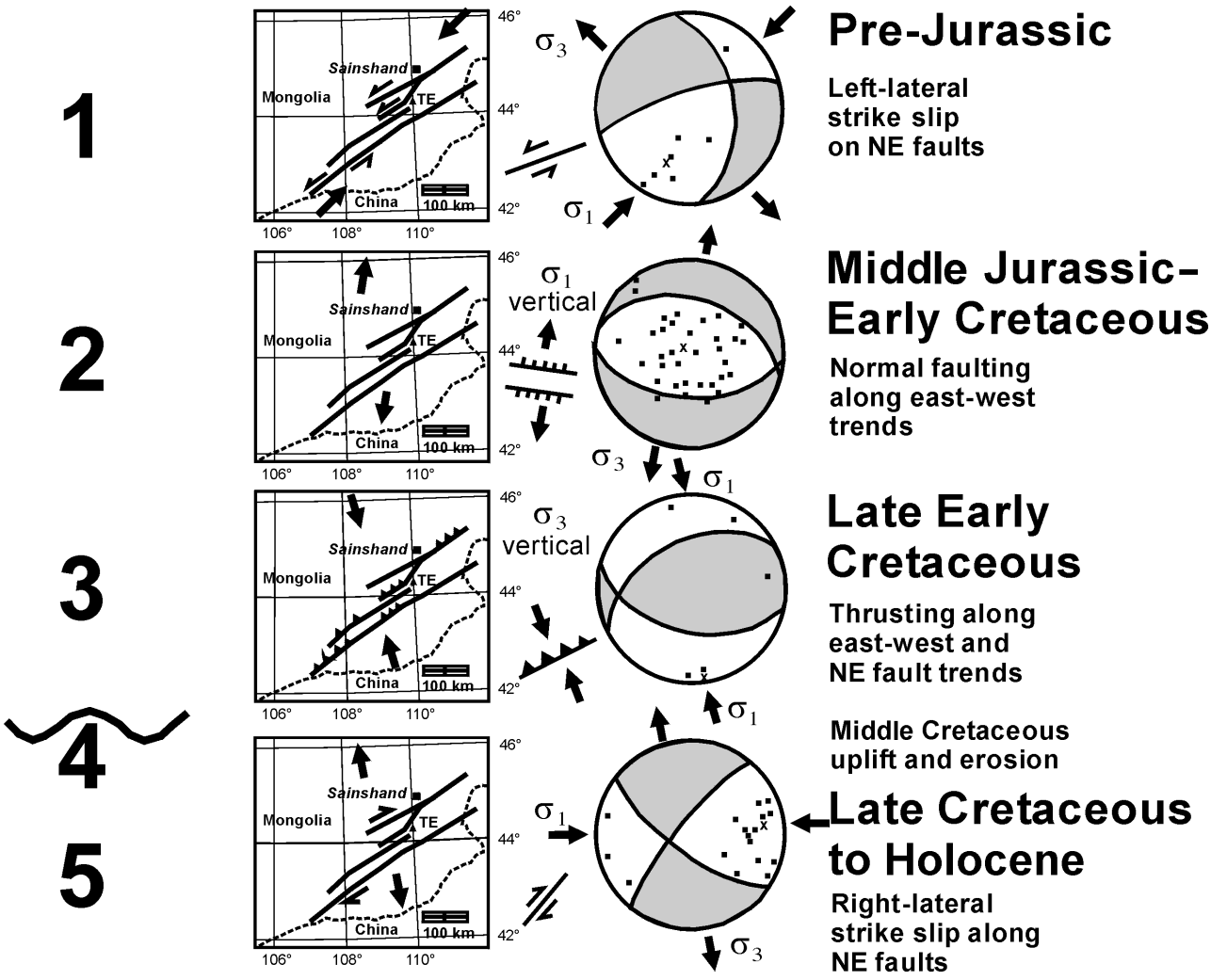

Figure 12. Summary diagram of kinematics measurements and the five proposed tectonic episodes that have affected the East Gobi basin.

to east-west since the Jurassic are a result of the changing influence of collision along the southern and Pacific margins of Asia. Paleomagnetic work shows that the tectonic development of Mongolia and north China is related to evolution of the Pacific plate (Pruner, 1992; Zhao et al., 1994, 1996). Despite the distances involved, north-south shortening resulted from the India–Asia collision, whereas east-west shortening was related to backarc spreading in the Sea of Japan (Rapp et al., 1985; Hefu, 1986).

Field mapping and seismic lines indicate that the anticline at Zuunbayan field is a northeast-trending and northwest-verging fold. This post-middle Cretaceous structure has a near-vertical to overturned northwestern flank (Figure 15), and units appear on seismic lines to thicken toward the fault (Figure 13A). Seismic data (line 92-41) show that this fold is formed by inversion over a preexisting normal fault, although the fault is not exposed at the surface. In general, folds associated with northeast– to east-northeast–trending and southeast-dipping faults should have gentle southeastern flanks and near-vertical to slightly overturned northwestern flanks (Figure 16).

The pre-Late Cretaceous Tsagaan Els field structure is a folded and tilted fault block with a hydrocarbon accumulation along the high edge of the block. Flattening on a horizon at the top of the Lower Cretaceous section indicates that this structure was folded or tilted and normal faulted prior to the middle Cretaceous unconformity (Figure 14B).

Folds near Khamaryn Khural, northeast of Zuunbayan, also trend northeast, have steep to overturned northwest flanks, and gentle southeastern flanks. Conversely, folds near Hutuul Uus, along the northern edge

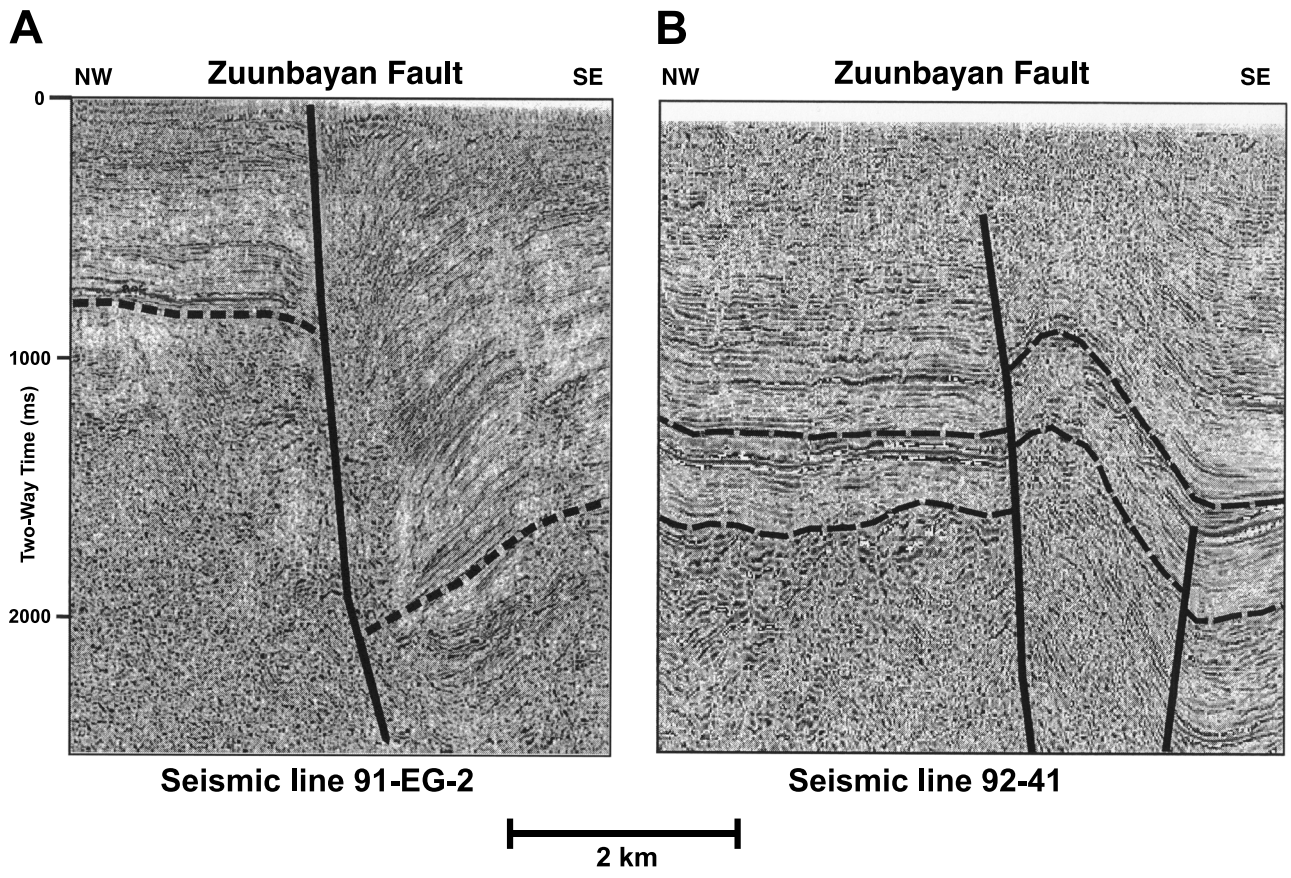

Figure 13. Seismic lines across the Zuunbayan fault. (A) Line 91-EG-2 shows normal offset southwest of the Zuunbayan field; (B) line 92-41 shows reverse offset west of the Tsagaan Els field. In these examples, the Zuunbayan fault displays early extension followed by inversion.

of the basin, verge to the south, and at least one at Unegt dome is almost circular, suggesting diapirism (Figure 4). This feature has no gravity signature (W. A. Jamieson, 1998, personal communication), and, other than gypsum veins (Table 2), evaporites have not been reported in the area. This fold may be shale cored.

The southern flank of the Sainshand basin is characterized by both symmetric and southeast-verging folds, which may have formed by inversion over northwest-dipping faults (Figure 6).

HYDROCARBON SYSTEM

An understanding of the structural style and timing of structural development is critical to modeling generation and migration of hydrocarbons. Extension and resultant accommodation space determine burial history, whereas timing of folding, tilting, and erosion dictate which structures can trap future hydrocarbons.

The burial history of the basins adjacent to the Zuunbayan and Tsagaan Els fields was modeled using available structure, well, and outcrop data. Data used in modeling included unit thickness, depth, kerogen type, total organic carbon (TOC), maturity as percent vitrinite reflectance (R_o), and temperature gradients. Twenty-eight wells were used, and twenty-nine pseudowells were created from well and outcrop sections. Pseudowells provide control points where real wells do not exist, namely, around the basin margins and in the basin center.

Hydrocarbon generation and expulsion was modeled using BasinMod 1-D, BasinView, and BasinFlow programs (Platte River Associates Inc., 1998). These programs take a stratigraphic section and heat-flow history from a well or basin and kinetic parameters based on kerogen type and source rock richness and apply kinetics equations to model the maturity, transformation ratio (percent of kerogen transformed to hydrocarbons), timing of generation, hydrocarbon type (oil vs. gas), and volumes generated.

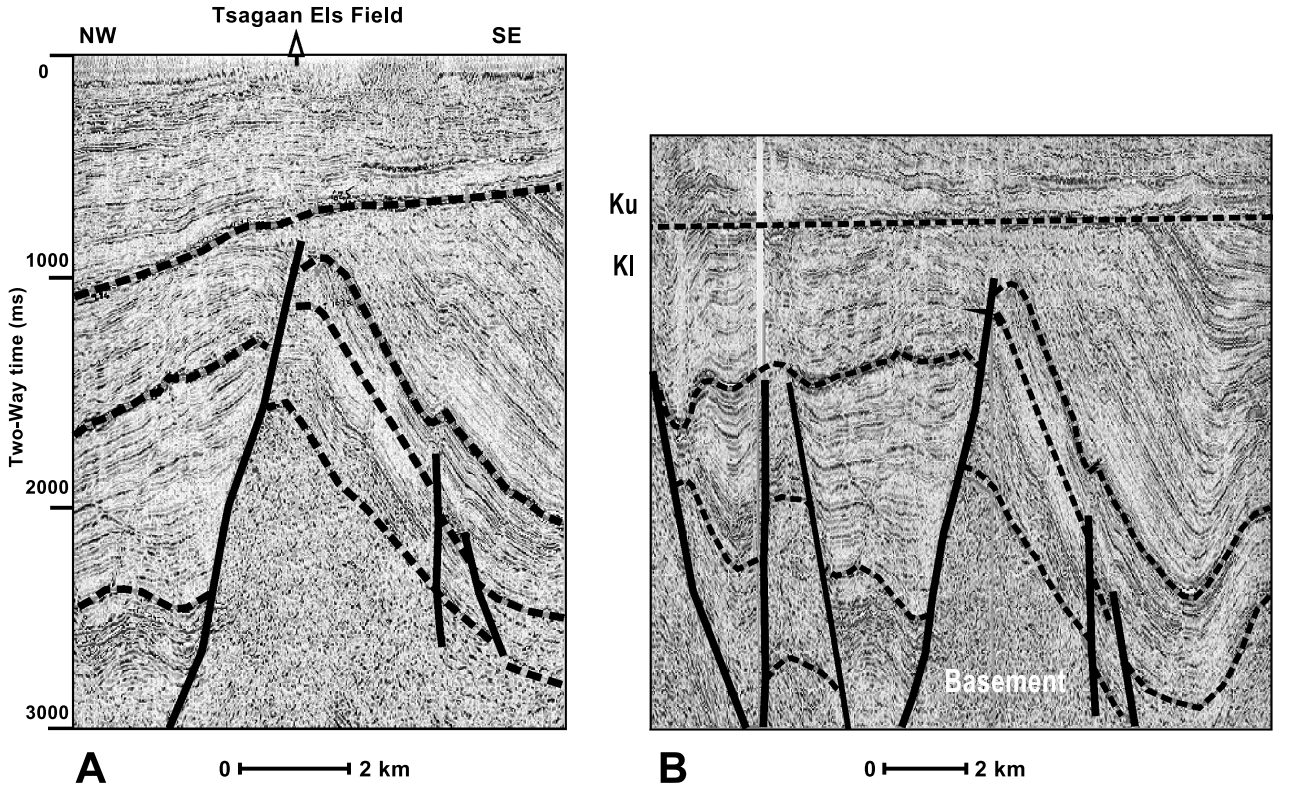

Figure 14. Line 91-EG-2 through the Tsagaan Els field. (A) This field is localized along the high edge of a tilted fault block. (B) Line 91-EG-2 flattened on the top Lower Cretaceous. This line illustrates both extension (tilted fault blocks) and shortening (thrusted kink fold on south flank Tsagaan Els structure) that occurred prior to the Late Cretaceous.

The results of modeling are strongly dependent on input parameters and assumptions made about the age and thickness of units, kerogen type, the amount of erosion at unconformities, previous surface temperatures, and heat-flow history.

Stratigraphic Data Used in the Model

Stratigraphic information (lithology, thickness, and tops) was taken primarily from the ''Report on the Mesozoic stratigraphy of the East Gobi basin, Mongolia'' (Lacustrine Basin Research Ltd., 1998, personal communication) and three tables of ''Deep wells around the Zuunbayan basin'' (D. Janchiv, 1998, personal communication). In the Unegt dome area, units and thicknesses were taken from the surface geologic map at 1:50,000 (Ositsev, 1951). In the Hutuul Uus area (northern Unegt subbasin), the units and thicknesses were taken from mapping by J. Amory of Stanford University (J. Y. Amory, 1997, personal communication). Near Khamaryn Khural (northeastern Zuunbayan subbasin), stratigraphic data is taken from Pershitkin et al. (1952).

Ages for local units are taken from ostracod biostratigraphy (Lacustrine Basin Research Ltd., 1998, personal communication) and from palynomorph zonation (E. H. Davies, 1999, personal communication). Radiometric age dating is used to assign ages to the Khamar Khavoor and Tsagaan Tsav formations and bituminous member (Graham et al., 2001; Johnson, 2002). Unit thickness and age was used to compile burial history curves at each well and pseudowell in the Unegt and Zuunbayan subbasins (Figure 17A).

Modeling burial history requires an estimate of the amount of section missing at unconformities. The amount of missing section affects source rock maturity: more missing section makes the subunconformity section more mature. Maturity calculated by BasinMod is compared to measured maturity (based on vitrinite reflectance) to calibrate the maturity vs. depth profile. The amount of missing section was estimated by measuring the amount of section eroded beneath unconformities or calculating the amount of section that

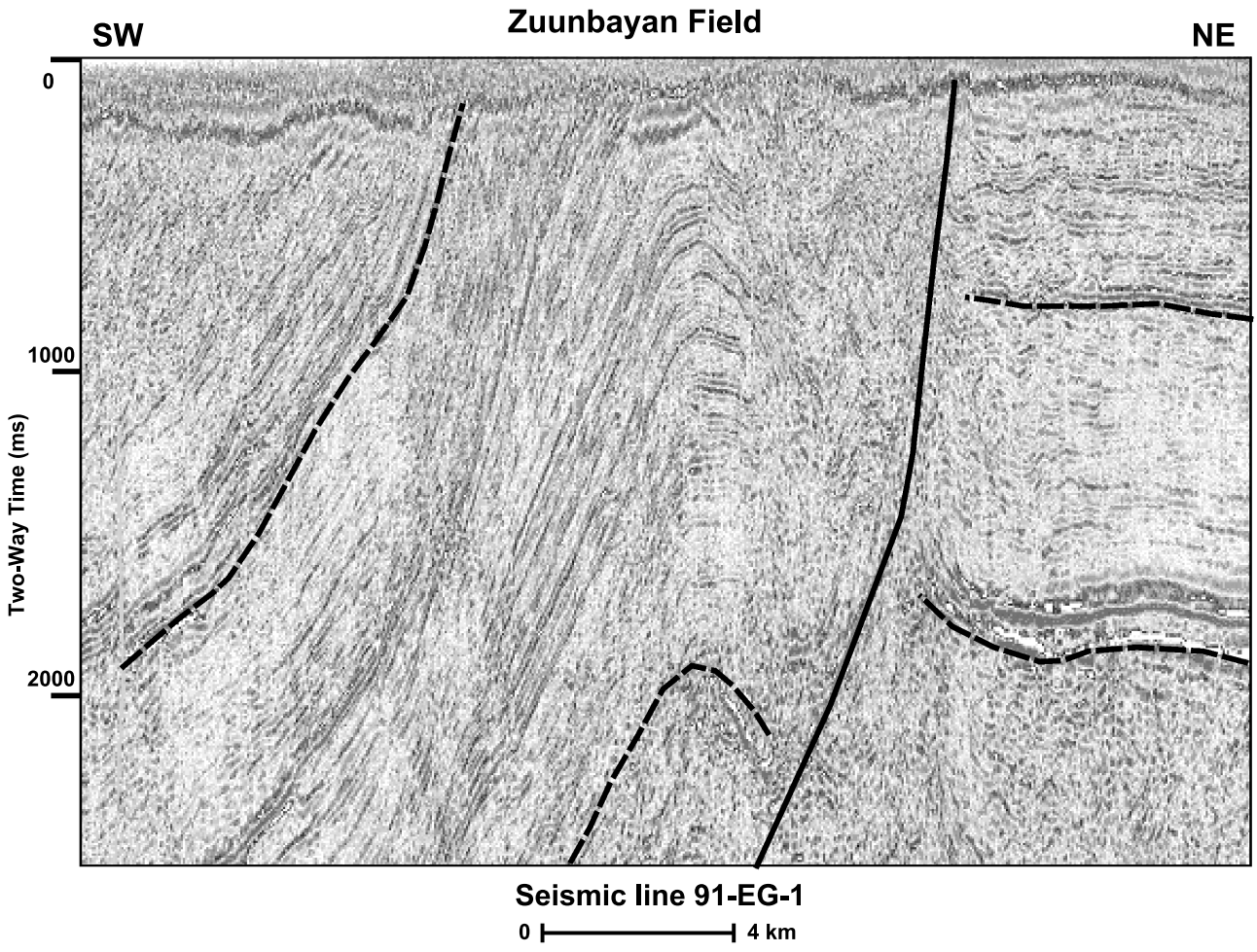

Figure 15. Southwest to northeast seismic line 91-EG-1 over the Zuunbayan field structure. This fold verges northwest and appears to be a result of structural inversion at a preexisting listric normal fault.

is needed to give the maturity seen in the sample using vitrinite samples from a well or outcrop.

The Sclater and Christie compaction method was chosen because it is applicable to clastic sequences (Platte River Associates Inc., 1998). This method is considered accurate for rapid rates of deposition, but may overstate porosities.

Reservoir

The primary reservoir in the East Gobi basin is the Lower Cretaceous (Valanginian) Tsagaan Tsav Formation. This series of shales and interbedded sandstones is the reservoir unit at the Tsagaan Els and Zuunbayan fields in the Unegt and Zuunbayan subbasins. Whether on outcrop or in drillers' cuttings logs, these sandstones are immature lithic arenites with a large component of volcaniclastics and cement-degraded porosity. Clean quartz arenites are expected to have better porosity and permeabilities. Satellite images were used to map granitic intrusives, such as those encountered at site 9-3-10 (north flank Togrog uplift; Figures 5, 10), with the expectation that sediments derived from these intrusives would have fewer lithic fragments and better porosity than elsewhere in the basin.

Coarse-grained sandstones in the producing Tsagaan Tsav Formation range from 13 to 18% porosity, with permeabilities in the range of 2–474 md (China National Petroleum Corporation, 1995). A possible secondary reservoir exists in sands of the Lower Cretaceous Zuunbayan Formation. Calculated porosities range from 5 to 18% and permeabilities from 0.25 to 16 md.

Isopachs of the Tsagaan Tsav Formation were generated from well data and, beyond areas of well control, were arbitrarily assigned based on average thicknesses

Table 2. Kinematic Data, Unegt and Zuunbayan Subbasins, East Gobi Basin

Faults Site	Fault	Strike (°)	Dip Direction (°)	Dip (°)	Sense	Rake (°)	Confidence (1 best; 3 worst)
98-9-3-9	F1	40	?	?	?	?	3
98-9-3-10	F1	22	292	72 NW	normal?	56 SW	3
	F2	38	128	71 SE	reverse	85 NE	2
98-9-3-11	F1	35	305	62 NW	right-lateral	3 SW	2
98-9-3-12	F1	300	210	85 SW	left-lateral	16 W	2
98-9-3-13	F1	65	155	43 SE	right-lateral	31 SW	2
	F2	65	155	35 SE	reverse?	90	3
	F3	75	165	27 SE	left-lateral	40 SW	3
98-9-3-14	F1	60	150	80 SE	?	?	3
98-9-4-1	F1	60	150	80 SE	normal	80 SE	2
	F2	80	170	70 SE	normal	65 SE	2
	F3	280	190	54 SW	normal	78 SE	2
98-9-4-2	F1	80	170	30 SE	normal	60 SW	1
	F2	330	60	41 NE	left-lateral, reverse	45 SE	1
	F3	285	195	45 SW	right-lateral, reverse	40 SE	1
	F4	82	352	38 NW	normal	55 NW	1
	F5	55	145	63 SE	reverse, left-lateral	50 SW	2
	F6	75	165	62 SE	normal, right-lateral	50 SW	1
	F7	280	190	46 SW	normal	80 SW	1
98-9-4-4	F1	75	345	74 NW	reverse, right-lateral	50 NW	2
98-9-4-6	F1	320	230	70 SW	normal	80 SW	2
	F2	278	8	85 NE	right-lateral	10 NW	2
	F3	337	67	60 NE	normal	80 NE	2
	F4	340	70	52 NE	normal	55 SE	2
98-9-4-8	F1	336	246	57 SW	normal, left-lateral	45 SW	1
	F2	344	254	70 SW	normal, left-lateral	50 SW	1
	F3	314	224	54 SW	normal, left-lateral	48 SW	1
98-9-4-9	F1	90	180	77 S	normal	90	2
98-9-4-10	F1	340	250	72 SW	normal	55 SW	3
	F2	50	140	56 SE	normal	90	3
	F3	10	300	42 NW	normal	65 NW	3
98-9-4-15	F1	320	230	67 SW	normal	70 SW	3
	F2	331	61	84 NE	normal	75 NE	3
	F3	310	220	80 SW	normal	60 SW	3
98-9-5-3	F1	278	8	87 NE	normal	60 NW	3
	F2	67	337	79 NW	normal	80 NE	2
	F3	306	36	81 NE	normal	82 NW	3
	F4	70		90	normal		3
98-9-5-4	F1	314	224	85 SW	left-lateral	15 SE	2
	F2	298	208	70 SW	normal	60 SW	2
	F3	60	150	65 SE	right-lateral	12 SW	1
	F4	80	170	82 SE	normal	?	3
98-9-6-1	F1	310	220	65 SW	reverse	75 SE	3
	F2	62	152	60 SE	normal	?	3
	F3	58	328	76 NW	normal	?	3
	F4	300	30	70 NE	normal	80 E	3

Table 2. (Continued).

Faults Site	Fault	Strike (°)	Dip Direction (°)	Dip (°)	Sense	Rake (°)	Confidence (1 best; 3 worst)
	F5	58	148	71 SE	right-lateral	0	2
	F6	55	325	62 NW	right-lateral	25 NE	3
	F7	74	344	86 NW	right-lateral	0	3
	F8	77	167	84 SE	left-lateral	15 SW	2
98-9-6-3	F1	56	326	65 NW	right-lateral	25 NE	2
	F2	58	328	75 NW	left-lateral	20 SW	2
	F3	64	334	68 NW	left-lateral, normal	40 SW	2
	F4	62	332	60 NW	normal	60 SW	2
	F5	61	151	78 SE	right-lateral	15 NE	1
98-9-6-4	F1	90	180	84 S	left-lateral	84 E	1
	F2	82	172	90	left-lateral	20 E	1
98-9-6-6	F1	48	318	46 NW	right-lateral	30 NE	2
	F2	65	335	85 NW	right-lateral	25 NW	2
	F3	60	330	47 NW	left-lateral, reverse	45 NE	2
	F4	25	115	80 SE	left-lateral	30 NE	2
	F5	52	322	80 NW	normal	75 NE	2
98-9-7-1	F1	14	284	89 NW	reverse	75 NE	1
98-9-7-2	F1	300	210	52 SW	left-lateral	9 SE	1
	F2	22	112	74 SE	normal	75 NE	2
	F3	4	94	54 SE	normal	51 NE	1
	F4	48	318	66 NW	normal	36 NE	3
98-9-7-3	F1	295	205	85 SW	normal, left-lateral	50 S	1
	F2	80	170	78 SE	normal	70 SW	1
	F3	275	185	86 SW	right-lateral	10 W	2
	F4	35	305	75 NW	norm, right-lateral	45 NE	3
	F5	44	134	73 SE	right-lateral	12 E	2
	F6	28	298	70 NW	right-lateral	24 N	3
98-9-7-4	F1	318	228	30 SW	right-lateral, normal	45 SW	1
	F2	358	268	80 SW	right-lateral	35 S	2
	F3	30	300	87 NW	right-lateral	8 SW	2
	F4	22	292	77 NW	right-lateral	?	3
	F5	22	292	84 NW	right-lateral	3 N	2
Fold Axial Planes		Strike (°)	Dip Direction (°)	Dip (°)	Plunge (°)		
98-9-3-8	Fold 1	63	153	61 SE	34 SW		
	Fold 2	51	141	64 SE	23 SW		
98-9-4-12	Fold 1	80	350	62 NW	7 NE		
Veins		Strike (°)	Dip Direction (°)	Dip (°)	Mode	Filling	
98-9-5-2	V1	62	332	76 NW	opening	gypsum	
	V2	35	305	77 NW	opening	gypsum	
	V3	24	114	77 SE	opening	gypsum	

seen in nearby wells or outcrops. Porosities at pseudo-wells are calculated for each formation based on their lithology and the Sclater and Christie compaction method. Permeability is calculated using the Modified Kozeny-Carman method, which is dependent upon porosity and grain size.

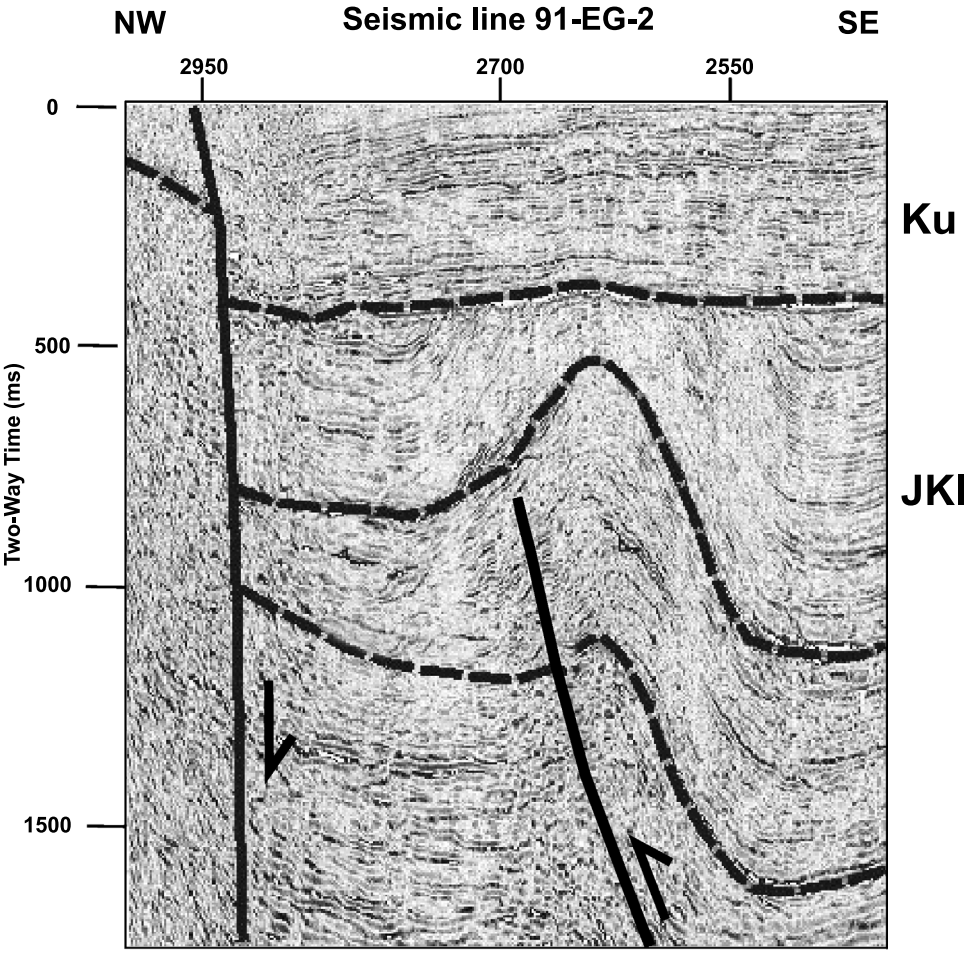

Figure 16. Seismic line 91-EG-2 along the northern edge of the Unegt basin shows undeformed Upper Cretaceous overlying thrusted folds in Lower Cretaceous and older units.

Source Rock

Lower Cretaceous mudstones are the probable source for hydrocarbons in the basin (Johnson, 2002). Isopachs of the bituminous member of the lower Zuunbayan Formation were generated from well data and, in areas without well control, were arbitrarily assigned based on average thicknesses seen in nearby wells or outcrops. Total organic carbon of the bituminous member ranges from 1.74 to 16.65% (average 7.9%) in outcrops (Phillips Petroleum Company and Mongolian Petroleum Company, 1992, personal communication) (Table 3). A value of 4% TOC was considered reasonable and was applied to the bituminous member of the Zuunbayan Formation.

Kerogen type is a key input to kinetics reactions. Type I kerogen (lacustrine algal) was used for the kinetics calculations (Stratigraphic Services International et al., 1991; Yamamoto et al., 1993).

The potential for hydrocarbon generation (network potential) is equal to the sum of S_1 and S_2 from pyrolysis of immature samples. Values taken from pyrolysis (Geotech Technical Services Pty. Ltd., 1998a, personal communication) of samples from the Tsagaan Tsav Formation in the TE-A3 well (Tsagaan Els field) average 0.865 mg/g TOC (range from 0.78 to 0.95 mg/g TOC). These samples are mature, having a T_{max} of 439°C, but are not good source rocks, because the maximum TOC is 1.1% (Table 3). $S_1 + S_2$ values in the Zuunbayan Formation in the Sainshand anticline average 8 mg/g (Mongolian Petroleum Company and Exploration Associates International of Texas, 1990). Values from the Zuunbayan oil shale in the Shawart-ovoo deposit 200 km (120 mi) west of the Zuunbayan field have a network potential of 39.88 mg/g and range from 4.09 to 72.02 mg/g (Yamamoto et al., 1993). An average value of 2.9 mg/g is used for the bituminous member Zuunbayan Formation, based on East Gobi basin outcrop samples and those from the TE-A3 well (Table 3) (Mongol Petroleum Company, 1992, personal communication). If low, this value could underestimate the amount of hydrocarbon generated.

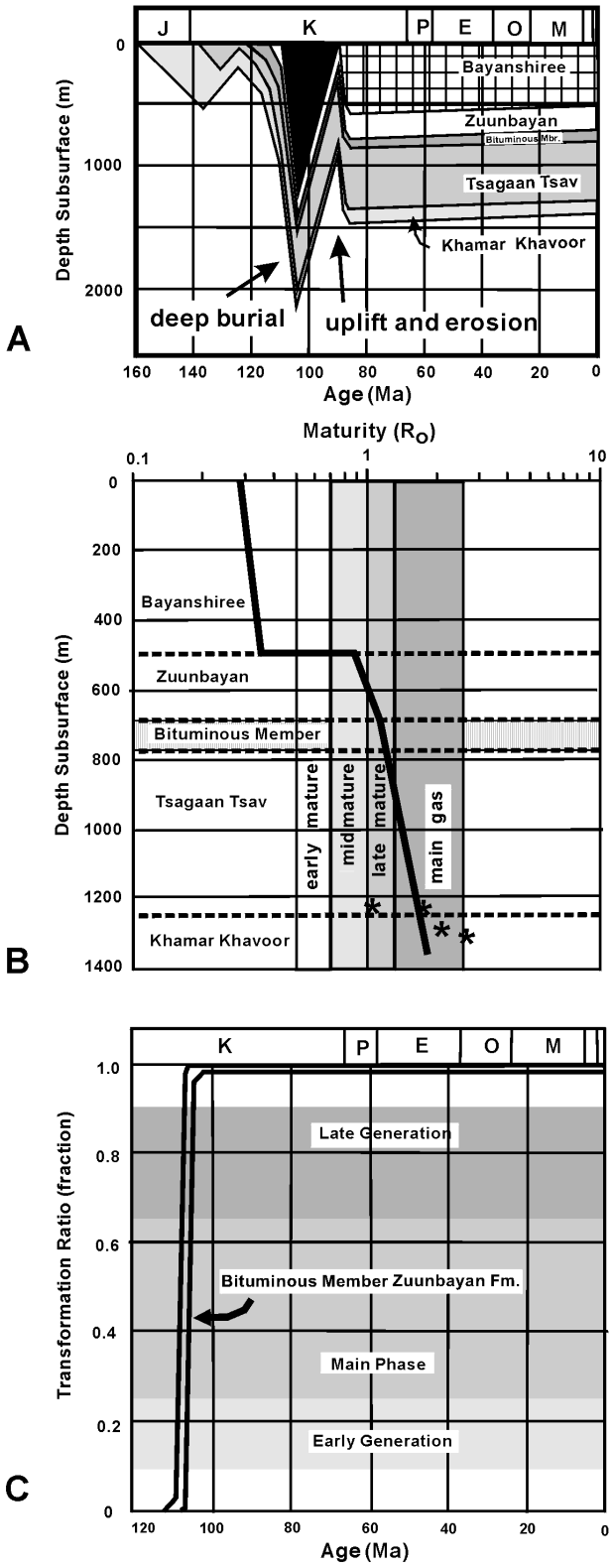

Figure 17. Modeling data for the TE-A1 well in the Tsagaan Els field. (A) Burial history curve. Note deep burial at 115–95 Ma and middle Cretaceous uplift and erosion. (B) Maturity vs. depth plot calibrated to vitrinite reflectance in well cuttings. The vitrinite reflection data (*) are a good fit, and the model suggests that the bituminous member of the Zuunbayan Formation is at the late mature (oil) stage. (C) Transformation ratio for the bituminous member. This ratio indicates how much of the kerogen in a source rock has been converted to hydrocarbon. Rapid burial between 105 and 113 Ma caused almost 100% of the kerogen to mature and generate hydrocarbons during that time interval.

Seal

Seals are provided by intraformational shales in the Tsagaan Tsav, Zuunbayan, and Sainshand formations.

Thermal History and Source Rock Maturity

A present-day average annual surface temperature of 4°C was used. This value comes from discussions of temperature with engineers and geologists at ROC Oil, which operates the Zuunbayan oil field. The surface temperature in the past was more temperate, and 20°C was used for paleosurface temperatures (S. Graham, 1999, personal communication).

Bottomhole temperatures (BHTs) were taken from the TE-A1, TE-A2, and TE-A3 wells and corrected by BasinMod for time since the end of mud circulation using Horner plots. The temperature gradient derived from BHTs in the TE wells is 4.5°C/100 m (2.47°F/100 ft). Bottomhole temperatures were used to calculate a present-day heat flow that averages 2.2–2.5 HFU (heat-flow unit) (1 HFU = 41.8 mW/m^2), consistent with heat flow in present-day rift environments. An average heat flow of 2.2 HFU (92 mW/m^2) for the region is considered reasonable and conservative and is used in the model.

Heat flow in the East Gobi basin has been estimated at 28 mW/m^2 or 0.67 HFU (Khutorskoy and Yarmoluk, 1989). This is much lower than heat flows suggested by BHTs and maturities seen near the Zuunbayan and Tsagaan Els fields. Five periods of igneous activity since 160 Ma are documented (Dobretsov et al., 1996). Measured maturity indicates moderately high heat flow during Jurassic–Cretaceous rifting (Johnson, 2002). Kerogen in the upper Tsagaan Tsav and lower Zuunbayan formations has been modeled as early-to-peak oil maturity, and models using a constant heat flow of 55 mW/m^2 (1.3 HFU) predict undermature source rocks (Johnson, 2002).

Thermal history in the model begins with a heat flow of 2.8 HFU at 300 Ma (Ordovician) declining to 2.6 HFU in the Early Cretaceous, then rising to three

Table 3. Total Organic Carbon, Maturity, and Rock-Eval Data for the Lower Cretaceous, East Gobi Basin*

Area (Reference)	Sample	TOC (wt.%)	$S_1 + S_2$ (mg/g)	T_{max}	R_o (%)	TAI
East Gobi Basin (Mongolian Petroleum Company and Exploration Associates International of Texas, 1990)						
Tsagaantsav Formation						
	6/1	0.31				
	6/2	1.23	58.00			
	6/3	0.38				
	6/5	1.48	33.00			
	6/7	1.47	25.00			
	6/8	7.70				
	7/2	0.33	27.00			
Lower Zuunbayan Formation						
	2/1	0.45				
	2/2	0.99				
	2/3	0.31				
	2/4	2.74	20.00			
	3/2	0.96				
	3/3	0.45	31.00			
	5/1	1.61	5.00			
	5/3	0.96				
Upper Zuunbayan Formation						
	4/1	0.30				
	4/2a	0.95				
	4/2b, c	0.74				
	4/3	0.29				
	4/6	1.40	11.00			
	4/7	0.17				
	4/8	0.39				
East Gobi Blocks XIV and XV outcrops (Mongol Petroleum Company, 1992)						
	167	2.61	3.66		0.40	2–
	168	3.18	5.24		0.40	2–
	169	1.01	0.47		0.44	2–
	170	0.90	0.22		0.41	2–
	171	2.98	5.14		0.40	2–
	172	2.61	4.46		0.41	2–
	173	1.58	2.08		0.39	2–
	174	2.88	4.64		0.40	2–
	175	3.10	4.50		0.40	2–
	189	0.59	0.12		0.42	2–
	193	0.53	0.16		0.38	2–
	382	4.66	5.34		0.45	2–
	383	1.30	0.31		0.47	2–
	384	0.66	0.13		0.47	2–
	385	1.84	1.06		0.45	2–
	386	2.59	3.87		0.46	2–
	387	4.66	6.75		0.46	2–
	388	6.15	13.09		0.45	2–
	389	1.43	0.39		0.48	2–

Table 3. (Continued).

Area (Reference)	Sample	TOC (wt.%)	$S_1 + S_2$ (mg/g)	T_{max}	R_o (%)	TAI
	390	2.04	2.53		0.42	2–
	391	1.74	2.50		0.44	2–
	392	4.31	9.79		0.49	2–
	393	2.06	1.33		0.47	2–
	394	1.74	1.36		0.48	2–
	464	1.10	0.22		0.43	2–
	1017	0.71	0.34		0.74	2+?
Eastern Mongolia (Phillips, 1992, personal communication)						
	85	14.82			0.31	
	86	16.65			0.32	
	88	13.45			0.35	
	89	8.87			0.41	
	90	13.14			0.32	
	390	2.04			0.42	
	391	1.74			0.44	
	392	4.31			0.49	
	393	2.06			0.47	
	394	1.74			0.48	
Shawart-ovoo (Yamamoto et al., 1993)						
	1	7.36	52.03	440		
	2	8.62	60.41	440		
	3	7.33	40.59	445		
	4	4.03	30.60	447		
	5	3.33	26.80	448		
	6	7.71	63.56	446		
	7	9.61	72.02	443		
	8	4.59	32.81	449		
	9	7.00	44.72	450		
	10	4.65	30.84	448		
	11	3.49	20.16	450		
	12	1.71	4.09	444		
TE-A3 well (Geotech, 1998a, b, personal communication)						
	Depth (m)					
	1325	0.27				
	1330	0.36			0.70	
	1335	0.22				
	1340	0.35				
	1345	1.10	0.95	439.00	1.52	
	1350	0.30				
	1355	0.24				
	1360	0.47	0.78	438.00	1.61	
	1365	0.38				
Outcrops, North Flank Unegt Basin (Core Laboratories, 1998, personal communication)						
	98-9-4-5				0.45	3/4
	98-9-4-9					3/4

Table 3. (Continued).

Area (Reference)	Sample	TOC (wt.%)	$S_1 + S_2$ (mg/g)	T_{max}	R_o (%)	TAI
TE-A1 well (E. H. Davies, 1999, personal communication)						
	Depth (m)					
	1220					3
	1240					3/4–
	1285					3/4–
	1305					4–
TE-A3 well (E. H. Davies, 1999, personal communication)						
	440					3/3+
	455					3/3+
	470					3/3+
	480					3/3+
	540					3/3+
	550					3/3+
	1075					3/4–
	1100					3/4–
	1135					3/4–
	1160					3/4–
	1175					3/4–
	1195					4–
	1250					3/4–
	1315					3/4–
	1370					3/4–

*TOC = total organic carbon; TAI = thermal alteration index.

highs corresponding to peaks of igneous activity (Dobretsov et al., 1996), and gradually declining to a present heat flow of 2.25 HFU.

Five new vitrinite samples were analyzed during this project: three from the TE-A3 well and two from outcrop samples. The well samples were in the Tsagaan Tsav Formation at depths of 1330, 1345, and 1360 m (4363, 4413, and 4462 ft) and showed midmature (0.73–1.53% R_o) to overmature (1.61–2.27% R_o) vitrinite (Geotech Technical Services Pty. Ltd., 1998b, personal communication). The outcrop samples are from the Lower Cretaceous Zuunbayan Formation and Jurassic Khamar Khoover Formation along the northern margin of the Unegt subbasin. Both samples showed R_o = 0.45% and spore color indicating immature source rock.

Thermal alteration index (TAI) is based on pollen color and is used as an adjunct to vitrinite reflectance to determine maturity of source rock. Values of 3 to 3+ (peak maturity for liquids and gas) and 4– (high maturity for gas; overmature for liquids) were obtained for the Zuunbayan and Tsagaan Tsav formations in the TE-A1 and TE-A3 wells (Table 3). Values of Batten 3/4 (immature) were determined for two outcrop samples of the Zuunbayan and Khamar Khoover formations from the northern flank of the Unegt subbasin (Core Laboratories, 1998, personal communication).

Vitrinite reflectance and TAI were used to calibrate the burial history and kerogen maturity vs. depth (Figure 17B). If calculated maturity was lower than measured maturity, then the amount of rock eroded at unconformities was increased until maturity calculated by the program matched measured maturity. Likewise, if measured maturity is lower than calculated maturity, then heat flow or the amount of rock eroded from above the outcrop should be decreased. These maturities are assumed to apply to source rock in the surrounding basin (Figure 18).

T_{max} is used to calibrate the temperature vs. depth curve. T_{max} values from pyrolysis of Tsagaan Tsav samples from the TE-A3 well (Geotech Technical Services Pty. Ltd., 1998a, personal communication) range from 438 to 439°C (Table 3). This is supported by T_{max} values from the Shawart-ovoo oil shale deposit 200 km

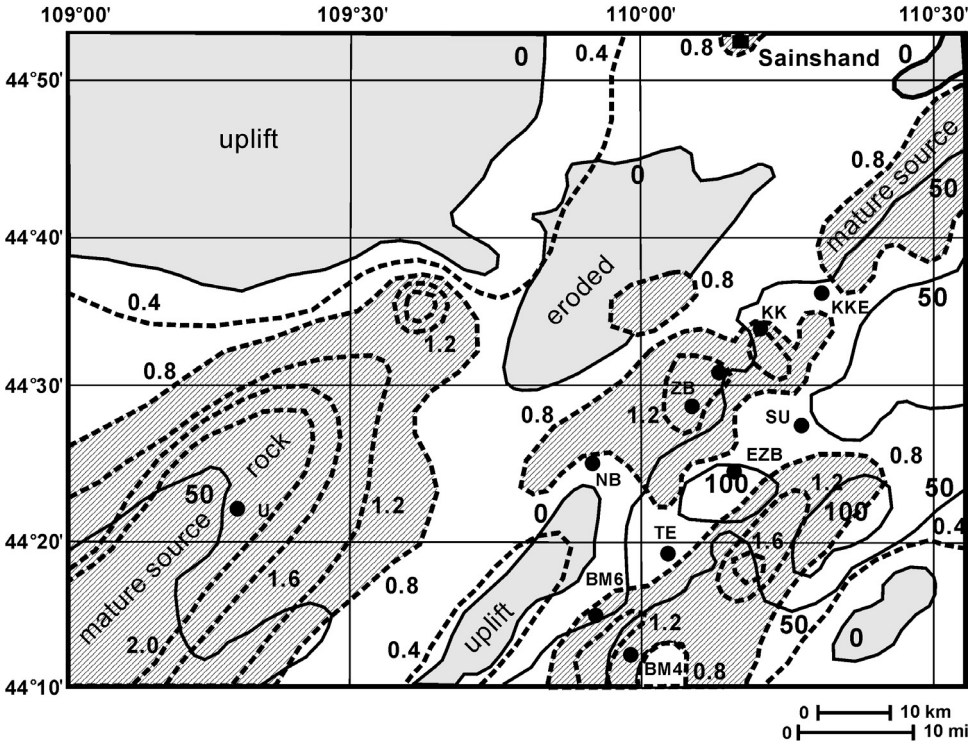

Figure 18. Isopach of the bituminous member of the Zuunbayan Formation, solid lines (50-m [164-ft] contour interval). Shaded areas are uplifts with no bituminous member present. Maturity of the bituminous member, dashed contours (0.4% R_o contour interval). Stippled area has R_o greater than 0.8, at least midmature source rock. Some of the well control is shown: BM4 = Bayan Mongol 4; BM6 = Bayan Mongol 6; EZB = East Zuunbayan; KK = Khamaryn Kural; KKE = Khamaryn Kural East; NB = New Bayanshiree; SU = South Ukhaa; TE = Tsagaan Els field; U = Unegt; ZB = Zuunbayan field.

(120 mi) west of Zuunbayan field: Values range from 440 to 450°C (Yamamoto et al., 1993).

Migration and Traps

Because seismic structure maps were not available, pseudowells were created to make the present-day structure and isopach maps conform more closely to what is known about the region. Pseudowells were generated to help define the basin margins and the undrilled basin centers that may have served as source kitchen areas.

Basement outcrop pseudowells were created where basement is at the surface. These wells effectively define the zero edge of basin fill. Basement pseudowells were distributed along the flanks of the basins. Basin center pseudowells were created to help define the deep parts of the basin (potential source kitchen), because actual wells are generally drilled on structural highs. The section used in these pseudowells is taken from the nearest well or measured surface section. Depth to top basement was derived from seismic lines using interval velocities. The real well or outcrop section was adjusted for calculated basement depth, and if space remained at the top, the Upper Cretaceous Sainshand or Bayanshiree Formation was added.

Structure maps are based on control at outcrops, wells, and widely spaced seismic lines. Pseudowells were created in the deep parts of basins and along basin margins to make the maps conform in a general way to what is known about basin geometry. The resulting structure contour map should be considered schematic. Still, structures exist where they are known to exist (Zuunbayan, Tsagaan Els, Unegt dome). The basin margins are where they should be, and deeps coincide with gravity lows and lows seen on seismic lines. BasinMod then simulated generation and migration of hydrocarbons updip under the influence of buoyancy, until they encountered traps or outcrop (Figure 19).

Structural traps observed at the surface and on seismic data include four-way fold closure in the form of domes (e.g., Unegt) and asymmetric anticlines (e.g., Zuunbayan), thrust-cored inverted folds, and tilted fault blocks (e.g., Tsagaan Els). Other potential trap types include faulted three-way closures and rollover on the downthrown side of listric normal faults. Potential stratigraphic traps include updip reservoir pinch-outs, updip subunconformity traps, tight gas sands and shales, and basin-centered gas accumulations.

Hydrocarbon Volume

Modeling shows that the bituminous member of the Zuunbayan Formation is mature over large parts of the Unegt and Zuunbayan subbasins and has probably generated substantial amounts of oil and some gas. Lack of a good structure contour map derived from seismic

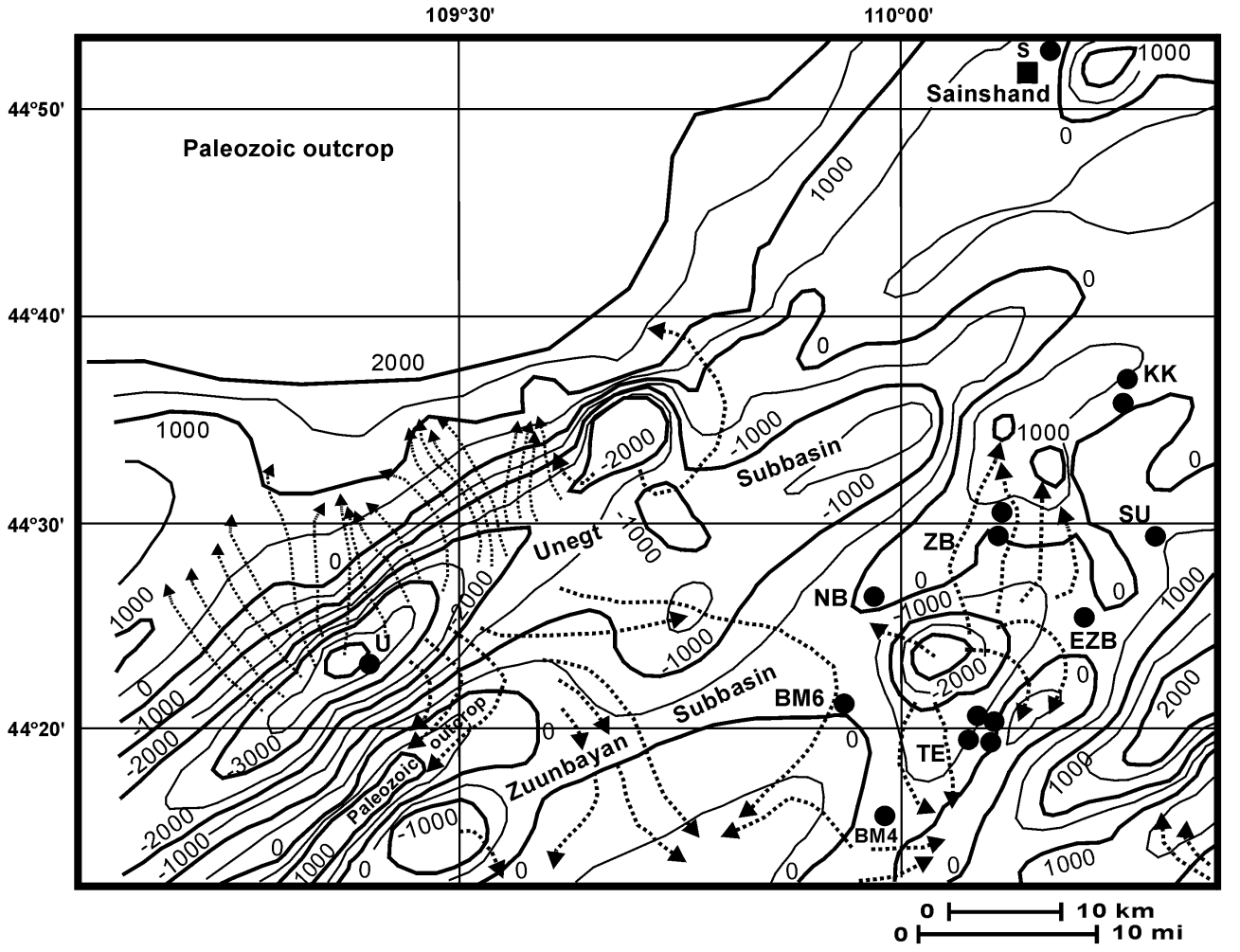

Figure 19. Migration paths and structure contours on the top of the Tsagaan Tsav Formation. Datum is sea level; 1000-m (3280-ft) contour interval. Migration paths are derived from the model by moving hydrocarbons updip perpendicular to strike. This figure shows that hydrocarbons moved out of the deep Unegt and northeast Zuunbayan subbasins toward the bounding uplifts and trapping structures (e.g., Zuunbayan, Tsagaan Els). Some of the well controls are shown: BM4 = Bayan Mongol 4; BM6 = Bayan Mongol 6; EZB = East Zuunbayan; KK = Khamaryn Kural; NB = New Bayanshiree; S = Sainshand; SU = South Ukhaa; TE = Tsagaan Els field; U = Unegt; ZB = Zuunbayan field.

data forced reliance on structure derived from wells, outcrops, and basin-center pseudowells. Not surprisingly, migration from the kitchen areas toward several traps, including the Zuunbayan and Tsagaan Els fields, is indicated when the structure map is combined with the reservoir (Tsagaan Tsav Formation) isopach. The basin around Unegt dome apparently generated the most hydrocarbons, which would have migrated to structures in or flanking the Unegt subbasin. Lesser amounts are indicated in the Zuunbayan and Tsagaan Els area, and this oil migrated into these fields and surrounding basement uplifts. The lack of present-day seeps along outcrops bordering the Unegt and Zuunbayan subbasins may be attributed to timing (peak migration occurred during the Cretaceous), erosion (evidence of seeps has been destroyed), and/or weathering and biodegradation of hydrocarbons in the near surface.

Early oil (104–112 Ma) was generated in the Zuunbayan and Tsagaan Els area because of deep burial during the middle to Late Cretaceous. Peak generation in the Unegt and Zuunbayan subbasins occurred between 100 and 90 Ma, just before and after the middle Cretaceous unconformity (Figures 17C, 20). Generation continues at a decreasing rate to the present day. Thus, both pre- and postunconformity structures may contain oil, at least in the Unegt subbasin (and other areas where there has been deep burial since the middle Cretaceous unconformity).

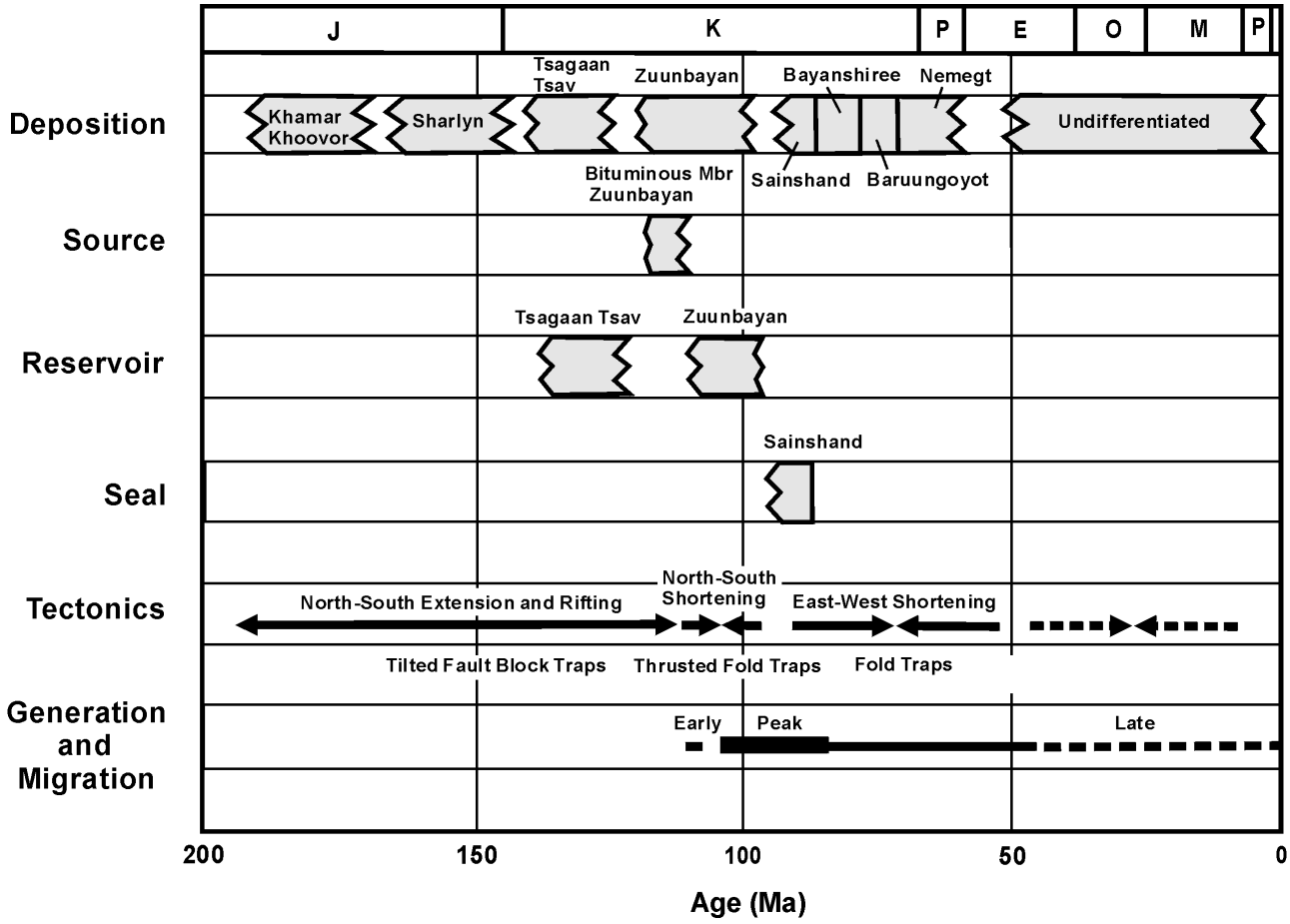

Figure 20. Hydrocarbon systems event chart. Peak oil generation and expulsion occurred between 113 and 85 Ma at a time when most structures already existed.

Modeling suggests that many structures are not filled to the spillpoint. This may or may not be the case and is a function of the (mostly conservative) parameters used: (1) source rock richness (conservatively set at 4% TOC), (2) source rock thickness (set at 1–50 m [3–164 ft] in the basin center), (3) heat-flow history and time of generation, (4) structural size as created from real and pseudowells, and (5) network potential (may be low at 2.8 mg/g TOC).

The volume of hydrocarbons generated is the most speculative product of basin modeling, because all assumptions and uncertainties are applied. Volumetric results should be viewed qualitatively instead of quantitatively, i.e., as indicating which areas are better than others. Volumes are highly dependent on structural geometry, which, in turn, is a function of well distribution instead of a well-defined seismic structure map. Still, a scoping calculation of volume of hydrocarbon generated suggests that the Unegt subbasin may have generated as much as 86 billion BOE; the area around Zuunbayan may have generated 15 billion BOE, and the area around Tsagaan Els may have generated as much as 10.8 billion BOE. Migration losses and oil or gas in place are not estimated. Kerogen maturities suggest oil is the most likely product over most of the subbasins.

CONCLUSIONS

The East Gobi basin consists of several large subbasins formed during Jurassic–Cretaceous rifting. Surface and subsurface mapping in the East Gobi basin suggests that the region has been subjected to at least five tectonic episodes: (1) pre-Jurassic northeast-directed shortening and left-lateral offset along east-northeast trends; (2) Middle Jurassic to Early Cretaceous rifting that formed elongated northeast-trending subbasins; (3) late Early Cretaceous shortening and inversion characterized by

left-lateral oblique reverse faulting along northeast trends; (4) middle Cretaceous uplift and erosion; (5) east-west shortening and right-lateral offset along northeast-trending faults.

Folds formed by inversion over Middle Jurassic–Early Cretaceous northeast– to east-northeast–trending normal faults. Folds that developed over northwest-dipping faults verge southeast, whereas folds that developed over southeast-dipping faults verge northwest. The anticline at Zuunbayan field is a northeast-trending and northwest-verging fold. This post-middle Cretaceous structure developed by inversion over a southeast-dipping normal fault. The Tsagaan Els field occupies the high edge of a pre-Late Cretaceous folded and tilted fault block.

The primary reservoir in the East Gobi basin is the Lower Cretaceous (Valanginian) Tsagaan Tsav Formation. These fluviodeltaic sandstones are the reservoir at the Tsagaan Els and Zuunbayan fields in the Unegt and Zuunbayan subbasins. Sandstones are immature lithic arenites with a large component of volcaniclastics. A possible secondary reservoir exists in channel sands of the Lower Cretaceous Zuunbayan Formation.

The most likely source rocks are Hauterivian to Albian lacustrine shales in the bituminous member of the Zuunbayan Formation. The Zuunbayan Formation should be mature over large parts of the Unegt and Zuunbayan subbasins and has probably generated oil and some gas. Modeling suggests that early oil (104–110 Ma) was generated in the Zuunbayan and Tsagaan Els area during the Cretaceous. Peak generation in the Unegt subbasin occurred between 100 and 90 Ma, just before and after the middle Cretaceous unconformity. Generation continued at a decreasing rate to the present. Kerogen maturities suggest that oil is the most likely product. Scoping calculations of hydrocarbon volumes generated indicate that the Unegt basin may have generated as much as 86 billion BOE.

REFERENCES CITED

Amory, J. Y., and A. M. Keller, 1995, An evaluation of Permian terrestrial deposits as potential hydrocarbon source rocks, southern Mongolia (abs.): AAPG Annual Meeting Program, v. 4, p. 3A.

Blechner, M. H., 1990, Oil and gas developments in Far East in 1989: AAPG Bulletin, v. 74, p. 257–280.

Chen, Y., V. Courtillot, J. P. Cogne, J. Besse, Z. Yang, and R. Enkin, 1993, The configuration of Asia prior to the collision of India: Cretaceous paleomagnetic constraints: Journal Geophysical Research, v. 98, no. B12, p. 21,927–21,941.

China National Petroleum Corporation (CNPC), 1995, Oil potential prediction analysis for East Gobi basin in Mongolia—Correlation analysis between East Gobi basin/Tsagaan Els and Zuunbayan oil fields and Erlian basin/Aershan oil field: Huabei, China, Exploration and Development Institute of Huabei Oil Administration Research Institute of Petroleum Exploration and Development of CNPC, 43 p.

Davis, G. A., Z. Yadong, Z. Changhou, and X. Bei, 2000, The Mesozoic Fengning–Longhua and Jiaoqier fault zones, north China; new interpretations of controversial structures (abs.): Geological Society of America Abstracts with Programs, v. 33, no. 3, p. 49.

Dewey, J. F., S. Cande, and W. C. Pitman, III, 1989, Tectonic evolution of the India/Eurasia collision zone: Eclogae Geologicae Helvetiae, v. 82, no. 3, p. 717–734.

Dobretsov, N. L., M. M. Buslov, D. Delvaux, N. A. Berzin, and V. D. Ermikov, 1996, Meso- and Cenozoic tectonics of the central Asian mountain belt: Effects of lithospheric plate interaction and mantle plumes: International Geology Review, v. 38, p. 430–466.

England, P., and P. Molnar, 1990, Right-lateral shear and rotation as the explanation for strike-slip faulting in eastern Tibet: Nature, v. 344, p. 140–142.

Ermikov, V. D., 1994, Mesozoic precursors of the Cenozoic rift structures of central Asia: Bulletin des Centres de Recherches Exploration-Prouduction Elf Aquitaine, v. 18, p. 124–134.

Everett, J. R., O. R. Russell, R. J. Staskowski, S. P. Loyd, and V. M. Tabbutt, 1991, Regional tectonic synthesis of eastern Mongolian People's Republic (abs.): AAPG Bulletin, v. 75, p. 570–571.

Graham, S. A., M. S. Hendrix, D. G. Badarch, and D. Badamgarav, 1996, Sedimentary record of transition from contractile to extensional tectonism, Mesozoic, southern Mongolia: Geological Society of America Abstracts with Programs, v. 28, p. 68.

Graham, S. A., M. S. Hendrix, C. L. Johnson, D. Badamgarav, G. Badarch, J. Amory, M. Porter, R. Barsbold, L. E. Webb, and B. R. Hacker, 2001, Sedimentary record and tectonic implications of Mesozoic rifting in southeast Mongolia: Geological Society of America Bulletin, v. 113, no. 12, p. 1560–1579.

Hefu, L., 1986, Geodynamic scenario and structural styles of Mesozoic and Cenozoic basins in China: AAPG Bulletin, v. 70, no. 4, p. 377–395.

Hendrix, M. S., S. A. Graham, J. Y. Amory, L. Lamb, A. M. Keller, R. Barsbold, and D. Badamgarav, 1994, Interplay of Mesozoic tectonics and climate in central Asia: Implications for Mesozoic-sourced oil fields of northern China and Mongolia (abs.): AAPG Annual Meeting Program, v. 3, p. 169.

Hendrix, M. S., S. A. Graham, J. Y. Amory, and G. Badarch, 1996, Noyon Uul syncline, southern Mongolia: Lower Mesozoic sedimentary record of the tectonic amalgamation of central Asia: Geological Society of America Bulletin, v. 108, no. 10, p. 1256–1274.

Johnson, C. L., 2002, Sedimentary record of late Mesozoic extension, southeast Mongolia: Implications for the petroleum potential and tectonic evolution of the China–Mongolia border region: Ph.D. geology dissertation, Stanford University, 358 p.

Johnson, C. L., L. E. Webb, S. A. Graham, M. S. Hendrix, and G. Badarch, 2001, Sedimentary and structural records of late Mesozoic high-strain extension and strain partitioning, East Gobi basin, southern Mongolia, *in* M. S. Hendrix and G. A. Davis, eds., Paleozoic and Mesozoic tectonic evolution of central Asia: From continental assembly to intracontinental deformation: Geological Society of America Memoir 194, p. 413–433.

Khutorskoy M. D., and V. V. Yarmoluk, 1989, Heat flow, structure

and evolution of the lithosphere of Mongolia: Tectonophysics, v. 164, p. 315–322.

Lamb, M. A., and G. Badarch, 1997, Paleozoic sedimentary basins and volcanic-arc systems of southern Mongolia: New stratigraphic and sedimentologic constraints: International Geology Review, v. 39, p. 542–576.

Lamb, M. A., A. D. Hanson, S. A. Graham, G. Badarch, and L. E. Webb, 1999, Left-lateral sense offset of upper Proterozoic to Paleozoic features across the Gobi Onon, Tost, and Zuunbayan faults in southern Mongolia and implications for other central Asian faults: Earth and Planetary Science Letters, v. 173, p. 183–194.

Marrett, R. A., and R. W. Allmendinger, 1990, Kinematic analysis of fault slip data: Journal of Structural Geology, v. 12, p. 973–986.

Meyerhoff, A. A., and R. F. Meyer, 1987, Geology of heavy crude oil and natural bitumen in the USSR, Mongolia, and China, *in* R. F. Meyer, ed., Exploration for heavy crude oil and natural bitumen: AAPG Studies in Geology 25, p. 31–101.

Mongolian Petroleum Company, 1992, Bouger gravity, Quads L-49-XX, XXI, XXVI, XXVII, XXXIII, blocks XIV (Zuunbayan), XV (Tariach), scale 1:200,000, 5 sheets.

Mongolian Petroleum Company and Exploration Associates International of Texas, 1990, Petroleum potential of Mongolia, 116 p.

Ositsev, D. K., 1951, Geologic map of the Unegt Mountain area (in Russian), scale 1:50,000, 1 sheet.

Peltzer, G., and P. Tapponnier, 1988, Formation and evolution of strike-slip faults, rifts, and basins during the India–Asia collision: An experimental approach: Journal of Geophysical Research, v. 93, no. B12, p. 15,085–15,117.

Pentilla, W. C., 1994, The recoverable oil and gas resources of Mongolia: Journal of Petroleum Geology, v. 17, no. 1, p. 89–98.

Pershitkin, M. B., P. K. Kharchikov, and K. P. Mitrafanova, 1952, Geological map and structure map of the Khamaryn Khural area, Mongolia (in Russian), scale 1:25,000, 1 sheet.

Petroleum Authority of Mongolia, date unknown, Geologic map of the East Gobi basin, multiple sheets, 1:500,000.

Platte River Associates Inc., 1998, User manual for BasinMod petroleum system software: Online user help: ⟨www.support @platte.com⟩ (accessed on December 1998).

Pruner, P., 1992, Palaeomagnetism and palaeogeography of Mongolia from the Carboniferous to the Cretaceous— Final report: Physics of the Earth and Planetary Interiors, v. 70, p. 169–177.

Rapp, R. H., M. L. Zoback, H. Koide, F. J. Mauk, G. W. Moore, Y. Kinugasa, T. Simkin, L. Siebert, D. R. Soller, and R. D. Brown, 1985, Geodynamic map of the Circum-Pacific region, northwest quadrant, *in* G. W. Moore, ed., Geodynamic maps of the Circum-Pacific region: Circum-Pacific Council for Energy and Mineral Resources, scale 1:10,000,000, 1 sheet.

Stratigraphic Services International (SSI), Geochemical Laboratories of Norway, Exploration Associates International of Texas, and Mongolian Petroleum Company, 1991, The sedimentary basins of south-central Mongolia, v. 1 part 2: Guildford, Surrey, SSI, 200 p.

Tapponnier, P., and P. Molnar, 1977, Active faulting and tectonics in China: Journal of Geophysical Research, v. 82, no. 20, p. 2905–2930.

Tapponnier, P., G. Peltzer, and R. Armijo, 1986, On the mechanics of the collision between India and Asia, *in* M. P. Coward and A. C. Ries, eds., Collision tectonics: Geological Society (London) Special Publication 19, p. 115–157.

Traynor J. J., and C. Sladen, 1995, Tectonic and stratigraphic evolution of the Mongolian People's Republic and its influence on hydrocarbon geology and potential: Marine and Petroleum Geology, v. 12, p. 35–52.

Tseden, T., S. Murao, and D. Dorjgotov, 1992, Introduction to geology of Mongolia: Bulletin of the Geological Survey of Japan, v. 43, no. 12, p. 735–744.

Webb, L. E., S. A. Graham, C. L. Johnson, G. Badarch, and M. S. Hendrix, 1999, Occurrence, age, and implications of the Yagan-Onch Hayrhan metamorphic core complex, southern Mongolia: Geology, v. 27, p. 143–146.

Yamamoto, M., D. Bat-Erdene, P. Ulziikhishig, M. Enomoto, Y. Kajiwara, N. Takeda, Y. Suzuki, Y. Watanabe, and T. Nakajima, 1993, Preliminary report on geochemistry of Lower Cretaceous Dsunbayan oil shales, eastern Mongolia: Bulletin of the Geological Survey of Japan, v. 44 no. 11, p. 685–691.

Yanshin, A. L., 1989, Map of geologic formations of the Mongolian People's Republic: Moscow, Academia Nauka, scale 1:1,500,000, 1 sheet.

Yue, Y., and J. G. Liou, 1999, Two-stage evolution model for the Altyn Tagh fault, China: Geology, v. 27, p. 227–230.

Zhao, X., R. S. Coe, Y. Zhao, H. Wu, and J. Wang, 1990, New paleomagnetic results from northern China: Collision and suturing with Siberia and Kazakhstan: Tectonophysics, v. 181, p. 43–81.

Zhao, X., R. S. Coe, Y. Zhao, S. Hu, H. Wu, G. Kuang, Z. Dong, and J. Wang, 1994, Tertiary paleomagnetism of north and south China and a reappraisal of late Mesozoic paleomagnetic data from Eurasia: Implications for the Cenozoic tectonic history of Asia: Tectonophysics, v. 235, p. 181–203.

Zhao, X., R. S. Coe, S. A. Gilder, and G. M. Frost, 1996, Paleomagnetic constraints on the palaeogeography of China: Implications for Gondwanaland: Australian Journal of Earth Sciences, v. 43, p. 643–672.